Article

IL-1beta promotes the age-associated decline of beta cell function

Marianne Böni-Schnetzler, Hélène Méreau, Leila Rachid, ..., Kelly Trimigliozzi, Daniel T. Meier, Marc Y. Donath

marianne.boeni@unibas.ch

Highlights

Islets from aged mice have increased IL-1beta and decreased IL-1Ra expression

Islet immune cells are the source of increased IL-1beta expression during aging

Myeloid-cell-specific IL-1beta knockout preserves insulin secretion in aged mice

IL-1beta targets genes regulating insulin secretion and proliferation during aging

Article

IL-1beta promotes the age-associated decline of beta cell function

Marianne Böni-Schnetzler,[1,2,3,*] Hélène Méreau,[1,2] Leila Rachid,[1,2] Sophia J. Wiedemann,[1,2] Friederike Schulze,[1,2] Kelly Trimigliozzi,[1,2] Daniel T. Meier,[1,2] and Marc Y. Donath[1,2]

SUMMARY

Aging is the prime risk factor for the development of type 2 diabetes. We investigated the role of the interleukin-1 (IL-1) system on insulin secretion in aged mice. During aging, expression of the protective IL-1 receptor antagonist decreased in islets, whereas IL-1beta gene expression increased specifically in the CD45 + islet immune cell fraction. One-year-old mice with a whole-body knockout of IL-1beta had higher insulin secretion *in vivo* and in isolated islets, along with enhanced proliferation marker Ki67 and elevated size and number of islets. Myeloid cell-specific IL-1beta knockout preserved glucose-stimulated insulin secretion during aging, whereas it declined in control mice. Isolated islets from aged myeloIL-1beta ko mice secreted more insulin along with increased expression of *Ins2*, *Kir6.2*, and of the cell-cycle gene *E2f1*. IL-1beta treatment of isolated islets reduced *E2f1*, *Ins2*, and *Kir6.2* expression in beta cells. We conclude that IL-1beta contributes the age-associated decline of beta cell function.

INTRODUCTION

Aging is the strongest risk factor for numerous metabolic disorders, including cardiovascular disease and type 2 diabetes (T2D) (Chia et al., 2018). Historically, T2D was considered to be an age-related condition. Even healthy elderly people suffer from deteriorating glucose tolerance due to decreased insulin action in peripheral tissues and impaired homeostatic insulin secretion (Basu et al., 2003; De Tata, 2014; DeFronzo, 1981; Gumbiner et al., 1989; Ihm et al., 2007; Meneilly et al., 1999). Moreover, aging is also characterized by reduced renewal and proliferation across many tissues (Iozzo et al., 1999; Lopez-Otin et al., 2013; Munoz-Espin and Serrano, 2014). Beta cells, being highly specialized secretory cells, already have a very low turnover rate, which declines even further with aging (Meier et al., 2008; Teta et al., 2005; Tschen et al., 2009).

Different factors contribute to the deterioration of beta cell function and reduced proliferation in old age. These involve the accumulation of senescent beta cells (Aguayo-Mazzucato et al., 2017, 2019; Helman et al., 2016), reduced mitochondrial function and Ca^{2+} handling (Barzilai et al., 2012; Cree et al., 2008; Ribeiro et al., 2012), reduced expression of beta cell identity genes and the glucose transporter Glut2 (Ihm et al., 2007; Novelli et al., 2000), reduced telomere length (Guo et al., 2011), activation of nuclear factor κB (NF-κB) signaling in beta cells, and increased presence of inflamed and fibrotic islet vascular cells (Almaca et al., 2014; Janjuha et al., 2018).

A factor affecting both beta cell function and turnover is the proinflammatory cytokine and signaling molecule interleukin-1beta (IL-1beta) (Bendtzen et al., 1986; Böni-Schnetzler and Meier, 2019; Maedler et al., 2002; Mandrup-Poulsen, 1996). Its receptor, the interleukin-1 receptor 1 (IL-1R1, gene name *Il1r1*), is highly expressed in endocrine beta cells relative to other mouse tissues (Benner et al., 2014; Böni-Schnetzler et al., 2009), making beta cells a prime target for both physiological and pathological effects of IL-1beta (Bendtzen et al., 1986; Böni-Schnetzler and Meier, 2019; Dror et al., 2017; Hajmrle et al., 2016; Maedler et al., 2002; Mandrup-Poulsen, 1996). Moreover, a recent comparison of different mouse tissue resident macrophages by transcriptomics revealed that islet and colonic macrophages express much higher levels of IL-1beta and inflammasome *Nlrp3* transcripts than other tissue macrophages, even in the absence of a metabolic challenge (see Figure S3 of reference (Brykczynska et al., 2020)). Interestingly, islet macrophages are constitutively M1 polarized (Brykczynska et al., 2020; Calderon et al., 2015; Eguchi et al., 2012; Ferris et al., 2017); this points to chronic and sustained IL-1 activity in islets that could potentially impact beta cell function and mass during aging. IL-1 activity is mainly counterbalanced by the endogenous IL-1 receptor antagonist

[1]Endocrinology, Diabetes, and Metabolism, University Hospital of Basel, 4031 Basel, Switzerland

[2]Department of Biomedicine, Diabetes Research, University of Basel, 4031 Basel, Switzerland

[3]Lead contact

*Correspondence: marianne.boeni@unibas.ch

https://doi.org/10.1016/j.isci.2021.103250

(IL-1Ra, gene name *Il1rn*), which competitively blocks IL-1R1 activation. Deletion of IL-1Ra in beta cells decreases insulin secretion via targeting of *E2f1* and the potassium channel subunit *Kir6.2* and prevents beta cell mass expansion (Böni-Schnetzler et al., 2018).

Based on the prominent expression pattern and functionality of IL-1 family members in endocrine and islet immune cells we aimed to investigate their expression during aging and to examine the potential contribution of the IL-1 system to the age-associated decline of beta cell function.

RESULTS

Aging reduces beta cell function and alters IL-1 and cell-cycle gene expression in islets

Fifty-two-week-old male C57BL/6N mice showed impaired glucose disposal in an intraperitoneal glucose tolerance test (ipGTT) when compared with their glucose clearance at 16 weeks of age (Figure 1A). Young mice increased plasma insulin in response to the glucose bolus, whereas aged mice had increased fasting insulin but diminished stimulation by glucose (Figure 1B). Hence the ratio of insulin at 15 to 0 min was lower in aged than in young mice, reflecting impaired insulin secretion (Figure 1C). Mean body weight increased from 29.7 g at 16 weeks to 41.5 g at 52 weeks of age (Figure 1D). Thus, islets of aged mice did not mount a sufficient insulin response to maintain glucose tolerance. To investigate a potential involvement of IL-1 in the age-related decline of beta cell function, we examined whether expression of IL-1 family genes in islets isolated from 12-, 29-, 52-, and 67-week-old mice changed during aging. The C57BL/6N mice used for this age-trajectory stem from the same colony and were housed in the same room, and to avoid any bias during islet isolation, the islets of different age groups were isolated in parallel. Compared with islets from young 12-week-old mice, gene expression of *Il1b* was increased at 29 and 67 weeks of age. Expression of *Il1a*, which is lower than *Il1b* in islets (Böni-Schnetzler et al., 2018), declined with age along with a slight reduction of the receptor *Il1r1*. Importantly, the protective *Il1rn* expression was decreased starting at 29 weeks of age (Figure 1E), and this resulted in a shift toward an increased ratio of *Il1b* to *Il1rn* as early as 29 weeks of age (Figure 1F). In contrast, chemokine *Cxcl1* and the immune cell markers *Adgre1* and *Cd68* were decreased at 52 and 67 weeks of age (Figure 1G). Although expression of islet identity markers *Ins2* and *Pdx1* did not change, the potassium channel subunit *Kir6.2* was lower in islets from 52-week-old mice (Figure 1H). The cell-cycle genes *Mki67*, *E2f1*, *Ccna2*, and *Ccnd1* were already strongly reduced in islets from 29-week-old mice (Figure 1I).

IL-1 family gene expression is induced in islet immune cells in aging

To identify the cellular sources of the age-related changes in IL-1 family genes in islets, we used 12- and 52-week-old beta cell reporter mice (RIP-EYFP) and isolated beta cells, CD45 + immune cells, and all residual islet cells termed "rest cells" by FACS (Figure 2A). qPCR of the three FACS fractions confirmed that *Ins2* is mainly expressed in the YFP + fraction (Figure 2B), whereas there was no expression of *Adgre1* (murine macrophage marker; Figure 2C) and *Gcg* (Figure 2D) in the beta cell fraction. *Adgre1* was expressed in the CD45 + immune cell fraction, and *Gcg* was detected in the rest cell fraction (Figures 2C and 2D). *Kir6.2* was expressed in the beta and the rest cell fractions and tended to be lower (p = 0.057) in the beta cell fraction from aged mice compared with the beta cell fraction from young mice (Figure 2E). *Il1b* and *Il1rn* expression were significantly increased in islet immune cells with age, whereas *Il1r1* and *Il1a* showed a trend toward an increase. *Il1b* and *Il1a* expression were not detectable, and *Il1rn* and *Il1r1* expression were unchanged in the remaining cells (Figures 2F–2H). Expression of *Mki67*, *E2f1*, and *Ccnd1* were strongly reduced in FACS-purified beta cells, whereas it was variable in immune cells from 52-week-old mice compared with 12-week-old mice. *E2f1* and *Ccnd1* were decreased in the "rest cells" (Figures 2I–2K). We did not note a difference in mean yields of islet CD45 + cells per mouse from 12-week-old versus 52-week-old mice. Altogether, this shows that during aging *Il1b* gene expression is selectively induced in islet immune cells, whereas cell-cycle genes were reduced in islet beta and rest cell fractions.

Aged IL-1beta knockout mice have increased insulin secretion

To investigate whether there is a causal link between age-associated changes in IL-1 family gene expression, altered islet function, and glucose tolerance, we first used whole-body IL-1beta knockout (ko) mice and compared them with littermate wild-type (WT) mice at the ages of 24, 52, and 68 weeks. IL-1beta protein was absent in the circulation (Dror et al., 2017) and in cultured peritoneal macrophages of IL-1beta ko mice (Figure S1A). At 24 weeks of age, there was no difference in glucose tolerance in an ipGTT (Figures 3A and 3B), insulin secretion (Figures 3C and 3D), insulin tolerance (Figures 3E and 3F), and body weight
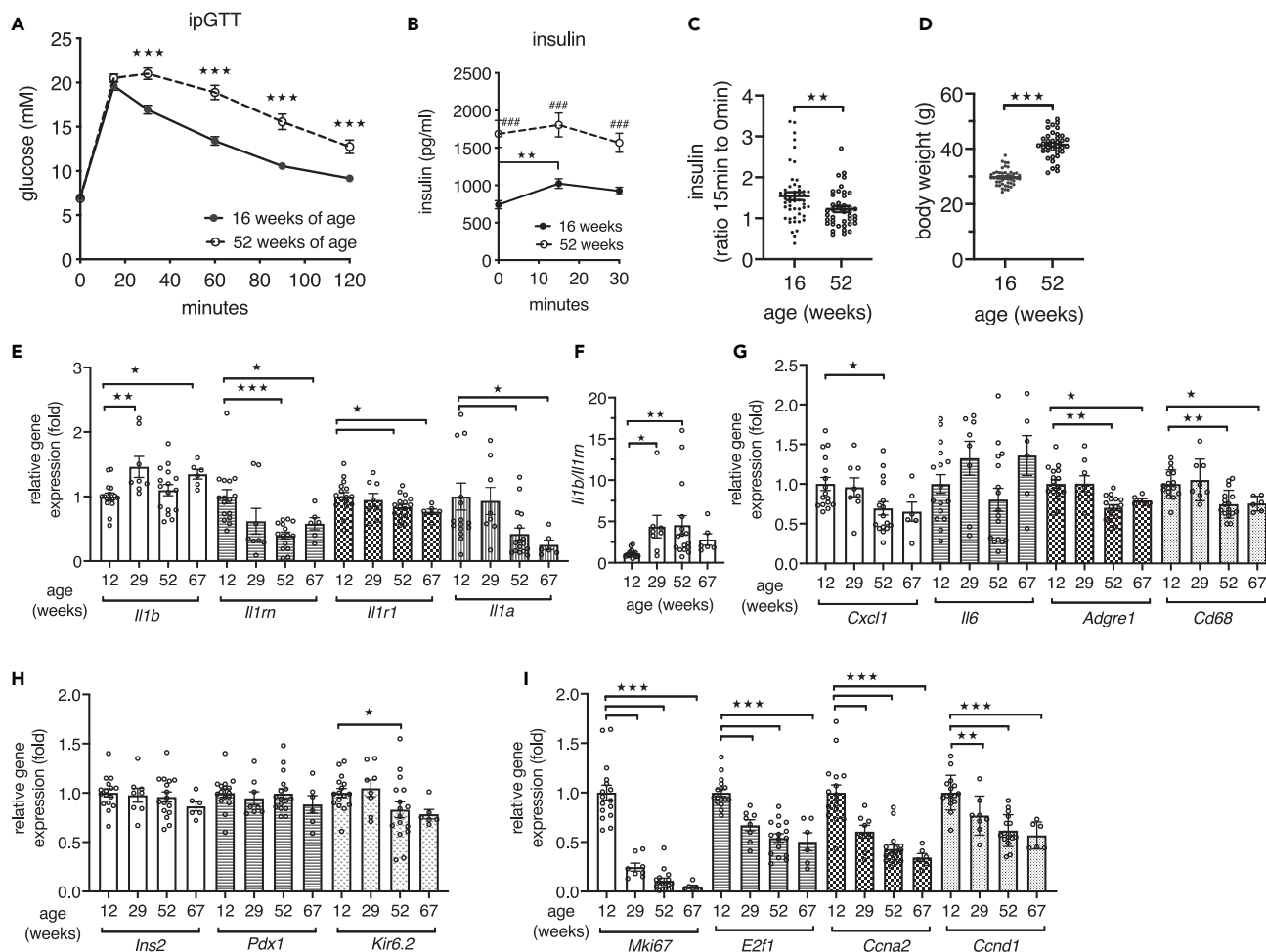
Figure 1. Aging leads to reduced beta cell function and altered IL-1 and cell-cycle gene expression in islets

(A) Plasma glucose concentrations during an ipGTT of male C57BL/6NCrl mice measured at the age of 16 weeks (n = 49) and again at the age of 52 weeks (n = 41).

(B) Corresponding plasma insulin concentrations during ipGTT.

(C) Ratio of plasma insulin at 15 min to 0 min of the ipGTT.

(D) Corresponding body weights of 16-week-old and 52-week-old male C57BL/6NCrl mice.

(E and G–I) Relative gene expression of islets isolated from male C57BL/6NCrl mice at the indicated ages; n = 16 mice at 12 and 52 weeks, n = 8 mice at 29 weeks, and n = 6 mice at 67 weeks.

(F) Ratio of relative gene expression of *Il1b* to *Il1rn*.

Statistics: (C and D) Student's t test; (E–I) one-way ANOVA and Sidak's multiple comparison test; error bars represent SEM, ★p < 0.05, ★★p < 0.01, ★★★p < 0.001. (A and B) two-way ANOVA and Sidak's multiple comparison test; (A) ★★★p < 0.001, 16 versus 52 weeks of age at the indicated time points; (B) ###p < 0.001, compares 16 weeks with 52 weeks at the indicated time points; ★★p < 0.01 compares 16-week-old mice at 0 min with 16-week-old mice at 15 min.

(Figure 3G) in IL-1beta ko versus littermate WT mice. At the age of 52 weeks, blood glucose during ipGTT was similar; however, circulating insulin levels of IL-1beta ko mice were strongly elevated compared with control mice (Figures 3H–3K). Possibly due to the elevated insulin levels, the body weight of IL-1beta ko mice was significantly higher, along with decreased insulin tolerance (Figures 3L–3N). Indeed, insulin release of 52-week-old IL-1beta ko mice positively correlated with body weight (Figures S1B and S1C). At 68 weeks, probably as a result of continued elevated insulin secretion (Figures 3Q and 3R), IL-1beta ko mice had an improved ipGTT relative to their respective littermate WT mice (Figures 3O and 3P), despite reduced insulin tolerance (Figures 3S and 3T) and a similar body weight (Figure 3U). Overall, these data revealed that in old age constitutive knockout of IL-1beta improves glycemia despite insulin resistance due to strongly elevated insulin release.
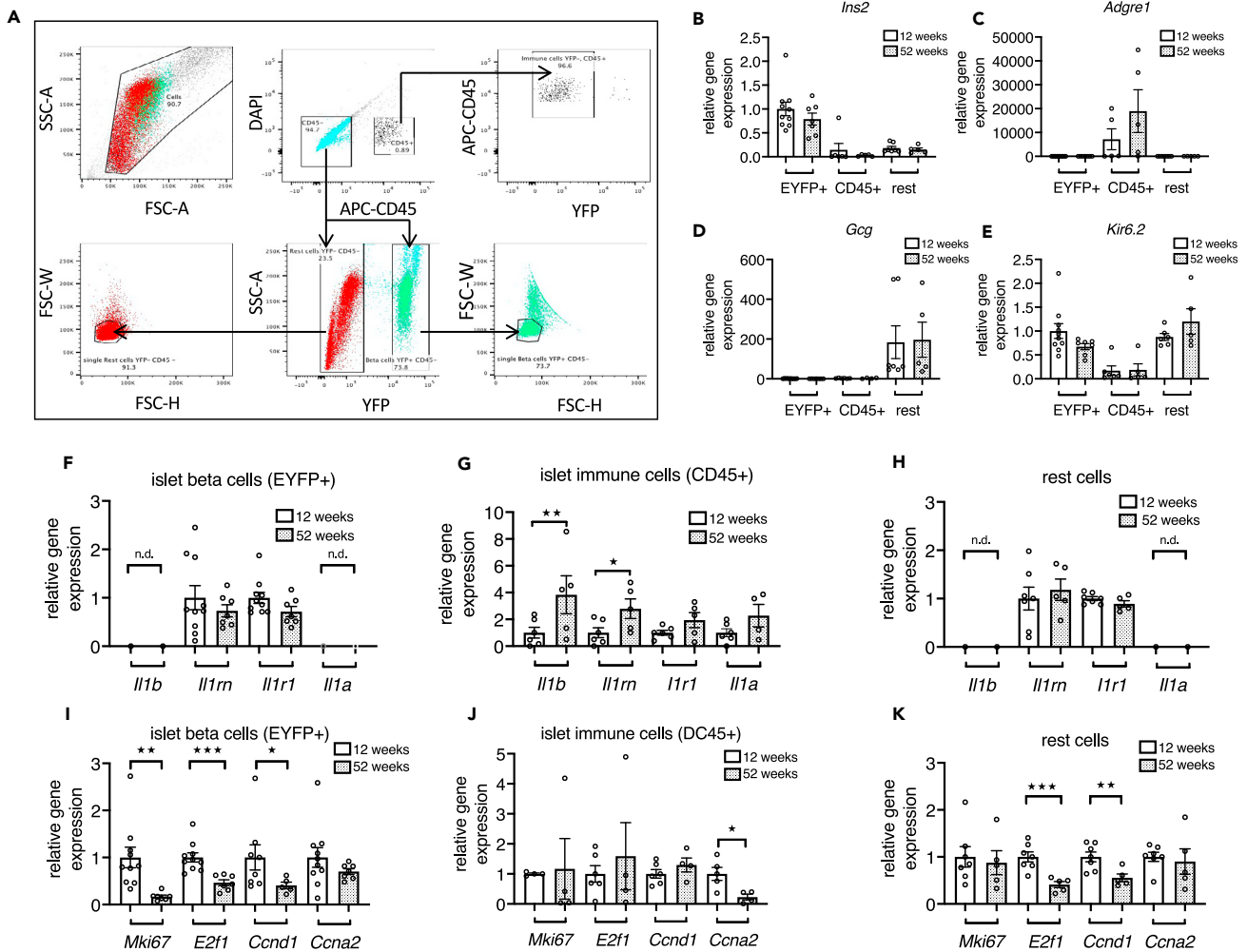
Figure 2. IL-1 family gene expression is induced in islet immune cells in aging

(A) Representative blots detailing the sorting strategy used for isolation of beta cell, rest cell and immune cell fractions from 12- and 52-week-old RIP-EYFP reporter mice. Upper panel: gating for Forward-Side Scatter Area (FSC-A/SSC-A) for bulk cells selection; size and granularity of beta cells (green) and rest cells (red) in sorted fractions; gating of CD45-negative and CD45-positive cells, DAPI was used to remove dead cells; sorting gate for the immune cell fraction based on CD45 positivity and YFP negativity. Lower panel: from the CD45-negative cell gate (upper middle blot), beta cells (green) were gated as YFP-positive cells and rest cells (red) as YFP-negative cells; single cell sorting gates for beta cells (right blot) and rest cells (left blot).

(B–E) Relative gene expression in all FACS fractions expressed as fold of mean expression level of EYFP+ cells from 12-week-old beta cell reporter mice.

(F–K) Relative gene expression of purified (F and I) beta cell, (G and J) islet immune cell, and (H and K) rest cell fractions from 12-week-old and 52-week-old mice, normalized to mean expression level of 12-week-old mice; n = 7–10 beta cell fractions, n = 5–6 immune cell fractions, and n = 5–7 rest cell fraction from 7–10 mice per age group (in case of low yield, immune cells or rest cells from 2 age-matched mice were pooled).

Statistics: Student's t test; error bars represent SEM; *p < 0.05, **p < 0.01, ***p < 0.001.

Deletion of IL-1beta increases insulin secretion and beta cell mass in aged mice

In vivo insulin secretion is modulated by many peripheral factors. To examine islet-intrinsic beta cell function, we isolated islets from 52-week-old IL-1beta ko and WT mice and measured glucose-stimulated insulin secretion (GSIS). Consistent with the observations *in vivo*, islets from aged IL-1beta ko mice had increased insulin release in response to 16.7 mM glucose (Figure 4A, for raw data see Figure S2A). The mean insulin content tended to be increased (Figure 4B, p = 0.086). The mean fold stimulation by high glucose (16.7mM glucose/2.8 mM glucose) was similar between IL-1beta ko and WT mice (Figure 4C), because both basal and glucose-stimulated insulin secretion were higher in islets of IL-1beta ko mice when data at high and low glucose concentrations were analyzed individually (Figures S2B and S2C). The mean islet yield per mouse was higher from IL-1beta ko mice than WT mice (Figure 4D). Next, we examined islet morphology in histological sections from IL-1beta ko mice. Mean beta cell mass was increased in
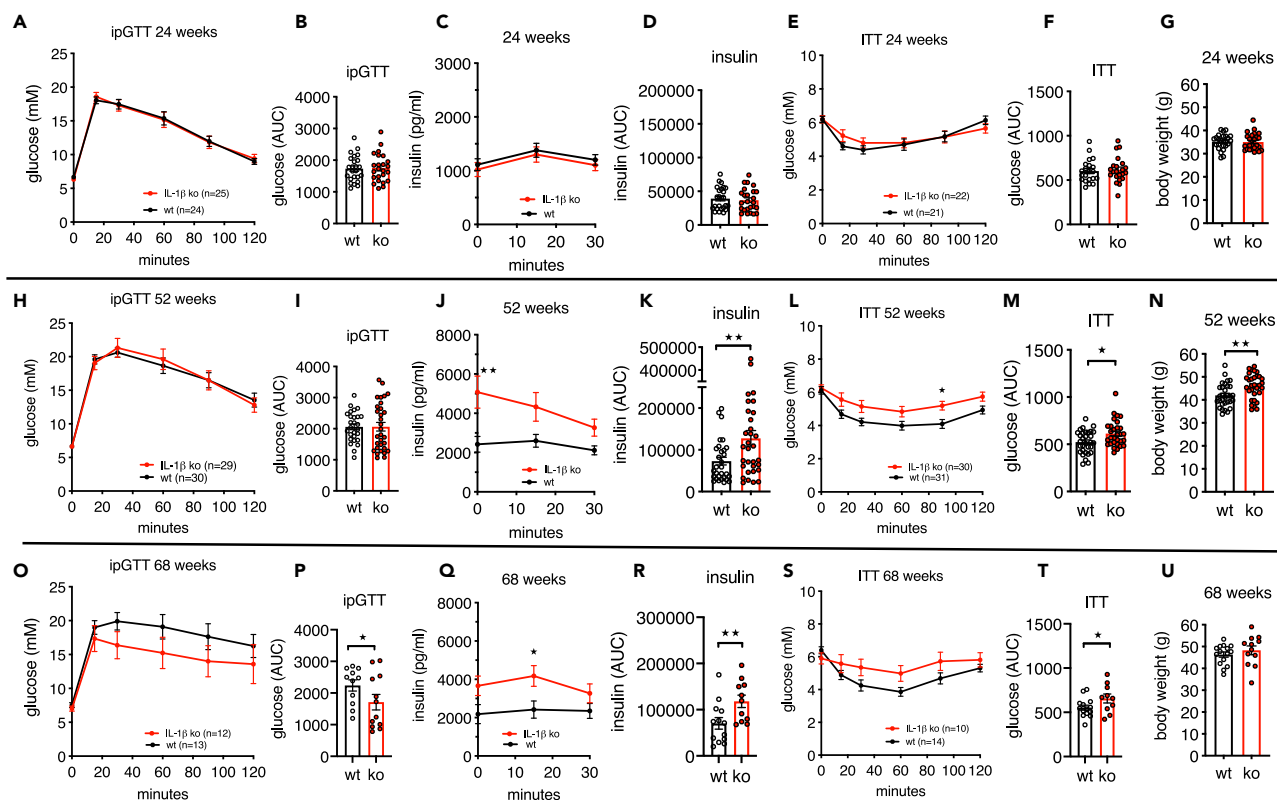
Figure 3. Aged IL-1beta knockout mice show increased insulin secretion

(A–G) 24-week-old IL-1beta ko mice (red) and littermate controls (black); (A and B) ipGTT and area under the curve (AUC) for glucose; (C and D) plasma insulin during ipGTT and AUC for insulin; (E and F) ipITT and AUC for glucose; (G) body weight.

(H–N) 52-week-old IL-1beta ko mice (red) and littermate controls (black); (H and I) ipGTT and area under the curve (AUC) for glucose; (J and K) plasma insulin during ipGTT and AUC for insulin; (L and M) ipITT and AUC for glucose; (N) body weight.

(O–U) 68-week-old IL-1beta ko mice (red) and littermate controls (black); (O and P) ipGTT and area under the curve (AUC) for glucose; (Q and R) plasma insulin during ipGTT and AUC for insulin; (S and T) ipITT and AUC for glucose; (U) body weight. Number of mice is indicated in figures.

Statistics: (A, C, E, H, J, L, O, Q and S) two-way ANOVA and Sidak's multiple comparison test; (B, D, F, G, I, K, M, N, P, R, T, and U) Student's t test; error bars represent SEM, *$p < 0.05$, **$p < 0.01$. See also Figures S1A–S1C.

52-week-old IL-1beta ko mice compared with age-matched controls and 24-week-old IL-1beta ko mice along with an increased mean islet area and number of islets per section. The beta cell mass of 52-week-old control mice was similar to the mass at 24 weeks of age (Figures 4E–4H). The islet size distribution of aged IL-1beta ko mice was shifted toward larger islets compared with controls (Figure 4I). IL-1beta ko mice had a higher percentage of islets with one or more beta cell(s) with nuclear Ki67 staining (Figure 4J), and the proportion of Ki67 + ins + cells was also higher when normalized to the mean islet area, although this did not reach statistical significance (Figure 4K). Altogether, these data suggested that during aging IL-1beta may act as a brake for the expansion of islet size and number.

We then compared gene expression of islets. As expected with a whole-body ko, *Il1b* mRNA expression was not detectable in islets from IL-1beta ko mice. Notably, there was no compensatory increase of *Il1a* gene expression in islets or liver, rather, *Il1a* was lower relative to controls (Figures 4L and 4N). Interestingly, gene expression of the protective *Il1rn* was higher in aged IL-1beta ko islets than in WT islets (Figure 4L), whereas circulating IL-1Ra levels were lower (Figure 4M) and *Il1rn* expression in the liver was similar (Figure 4N). Finally, in islets from aged IL-1beta ko mice, expression of the proliferation marker Ki67 (gene *Mki67*) and *Kir6.2* were increased compared with WT controls (Figures 4O and 4P).

Deletion of IL-1beta in myeloid cells preserved GSIS in aged mice

A major cellular source of IL-1beta in islets are macrophages, which constitute around 85% of all immune cells (CD45 + cells) present in mouse islets (Dalmas et al., 2017). Furthermore, the age-associated increase
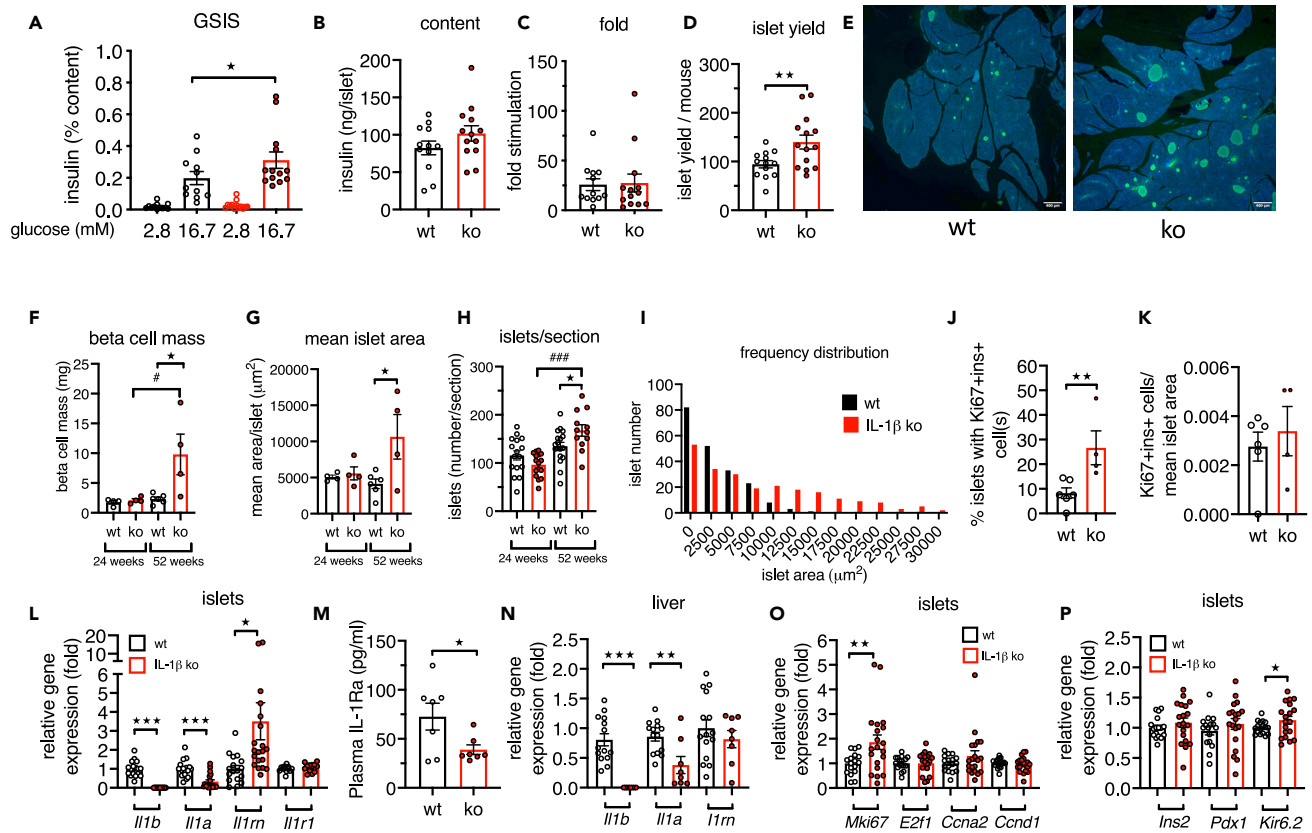
Figure 4. Deletion of IL-1beta increases beta cell mass and insulin secretion in isolated islets

(A–D) GSIS of isolated islets of 52-weeks-old IL-1beta ko (red) and littermate WT control (black) mice; (A) 1 h insulin secretion expressed as percentage of the insulin content per mouse; (B) insulin content per islet; (C) insulin fold stimulation by glucose, (mean of 4 × 10 islets per mouse); (D) number of islets isolated per mouse; n = 11–12 WT and n = 13–14 IL-1beta ko mice.

(E) Example of immunohistochemical staining of pancreata from IL-1beta ko and WT control mice (green = insulin, blue = DAPI, scale bar, 400 μm).

(F and G) Beta cell mass and mean islet area from 3–4 sections/mouse of 24- and 52-week-old WT and IL-1beta ko mice.

(H) Number of islets per pancreas section.

(I) Frequency distribution of islet area from 52-week-old IL-1beta ko mice and WT mice.

(J) Percentage of islets with one or more Ki67+/ins+/DAPI + cell(s); 472 islets from 4 IL-1beta ko mice and 509 islets from 6 littermate control mice were analyzed.

(K) Ki67+/ins+/DAPI + normalized to the mean ins + islet area.

(L, N–P) Relative gene expression of 52-week-old IL-1beta ko versus littermate WT control mice; (L and N) IL-1 family genes in islets and liver; (O) cell-cycle genes in islets; (P) islet genes. (M) Plasma IL-1Ra in 52-week-old IL-1beta ko and control WT mice. All data were expressed per mouse.

Statistics: (A, F-H) two-way ANOVA and Sidak's multiple comparison test; (B–D, and J–P) Student's t test; error bars represent SEM, ★p < 0.05, ★★p < 0.01, ★★★p < 0.001, #p < 0.05, ###p < 0.001. See also Figures S2A–S2C.

of *Il1b* was localized to islet immune cells (Figure 2G). We therefore used as a second *in vivo* model, the myeloid-cell-specific IL-1beta ko mice (*Lyz2 Cre$^{+/-}$_ Il1b$^{fl/fl}$*) and littermate WT controls (*Lyz2 Cre$^{-/-}$_ Il1b$^{fl/fl}$*) and examined their islet function and glucose homeostasis in aging. Knockout efficiency of *Il1b* expression in myeloIL-1beta ko mice was 96.3% in peritoneal macrophages, 94.8% in liver tissue, and 68% in islets (Figure 5A). At protein level, IL-1beta secretion by cultured peritoneal cells was strongly reduced (Figure S3A). As observed previously (Figures 2F–2H), *Il1b* was selectively expressed in CD45 + islet cell fractions, and hence the knockout occurred in these cell fractions (Figure 5B, FACS fraction controls see Figure S3B). We next examined glucose tolerance, insulin secretion, and insulin tolerance at 16, 24, and 52 weeks in the same cohorts of myeloIL-1beta ko and littermate control mice (Figures 5C–5H). At younger age (16 and 24 weeks) mice had similar insulin secretion profiles, whereas at 52 weeks of age myeloIL-1beta ko mice had a better glucose-stimulated insulin secretion than WT controls and increased AUC for insulin (Figures 5C and 5D). The ratio of insulin at time points 15 to 0 decreased with age in littermate controls, whereas it was preserved during aging in myeloIL-1beta ko mice (Figure 5E). Moreover, glucose
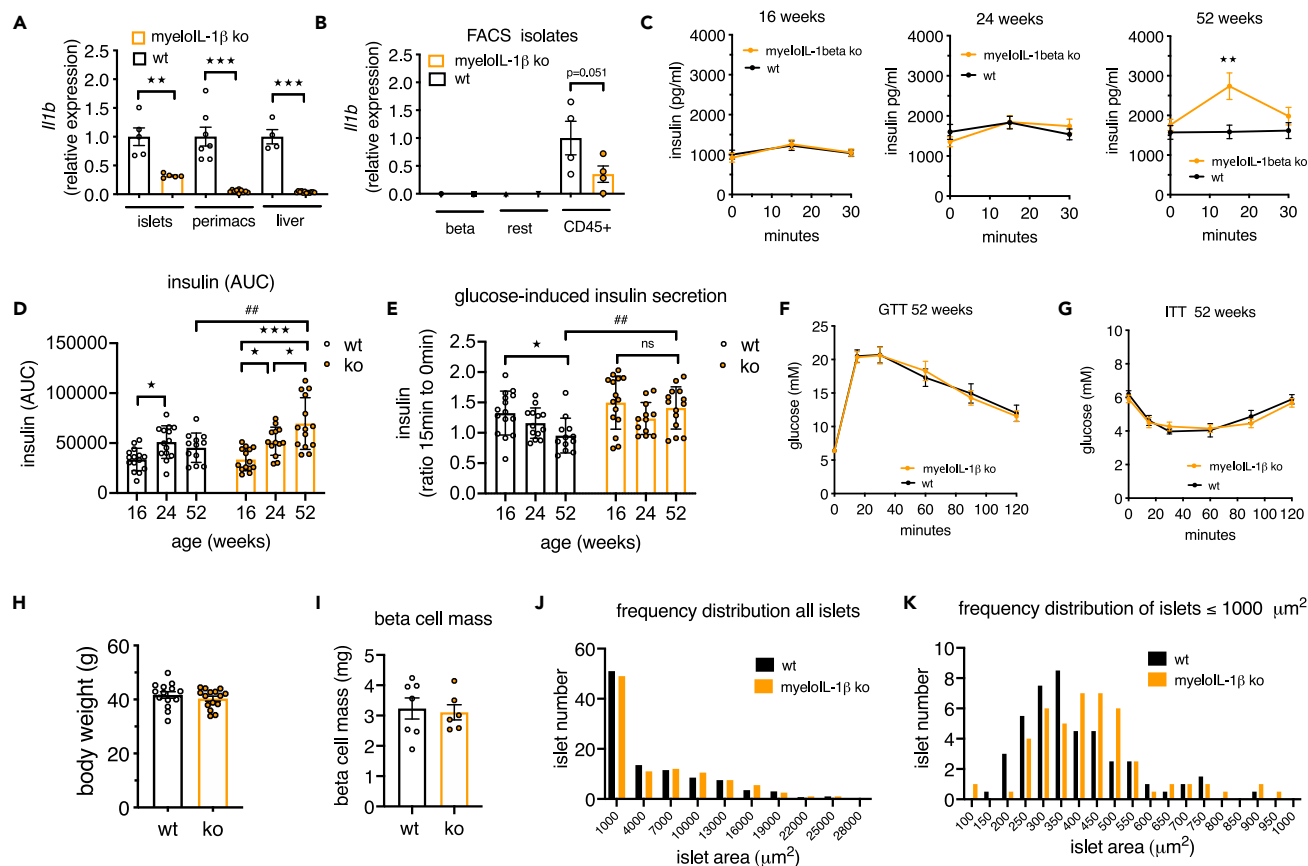
Figure 5. Deletion of IL-1beta in myeloid cells preserves GSIS in aged mice

(A) *Il1b* expression in islets, peritoneal macrophages (perimacs), and liver from myeloIL-1beta ko (orange) and control mice (black).

(B) *Il1b* expression in FACS-isolated islet cell fractions (n = 4, one data point stems from an islet pool of 2 mice, total 8 mice per genotype).

(C–H) Age trajectory of myeloIL-1beta ko mice (orange) and control mice (black); (C) *in vivo* glucose-stimulated plasma insulin of the same myeloIL-1beta ko (orange) and control mice (black) measured at different ages during ipGTT (n = 13–15 WT mice and n = 14–15 myeloIL-1beta ko mice from 2 separate cohorts); (D) area under the curve (AUC) of plasma insulin of the age trajectory; (E) ratio of plasma insulin at 15 min to 0 min during ipGTT of the age trajectory; (F) plasma glucose during ipGTT; (G) plasma glucose during ipITT; (H) body weight of 52-week-old mice.

(I) Beta cell mass determination.

(J) Frequency distribution of all islets in histological sections of 52-week-old myeloIL-1beta ko (n = 6) and control (n = 7) mice.

(K) Frequency distribution of islets zooming into islet area <1,000 μm^2.

Statistics: (A, B, H, and I) Student's t test; (C–G) two-way ANOVA and Sidak's multiple comparison test; error bars represent SEM, *p < 0.05, **p < 0.01, **p < 0.01, ***p < 0.001, ##p < 0.01; ns, not significant. See also Figures S3A, S3B, S4A, and S4B.

and insulin tolerance at 16, 24, and 52 weeks of age did not differ between ko and control mice (Figures 5F–5H and Figure S4A), pointing to an islet-intrinsic functional improvement in aged myeloIL-1beta ko mice. One-year-old Cre-only mice (*Lyz2 Cre+/−*) had no insulin or glucose phenotype compared with littermate controls (Figure S4B). Histological analysis of beta cell mass showed no differences between genotypes (Figure 5I). Analysis of islet size frequency distribution revealed that in islets with an area up to 1,000 μm^2, which constituted around 50% of all islets, there was a shift toward larger islets in myeloIL-1beta ko mice compared with controls (Figures 5J and 5K).

Deletion of IL-1beta in myeloid cells preserved beta cell function in isolated islets from aged mice

We subsequently isolated islets from 52-week-old myeloIL-1beta ko and littermate control mice and assessed *in vitro* insulin secretion. Islets from myeloIL-1beta ko mice had increased GSIS compared with islets from WT mice when normalized to the insulin content (Figure 6A, raw data Figures S5A and S5B), whereas the mean islet insulin content was not different (Figure 6B). An age comparison of aforementioned GSIS
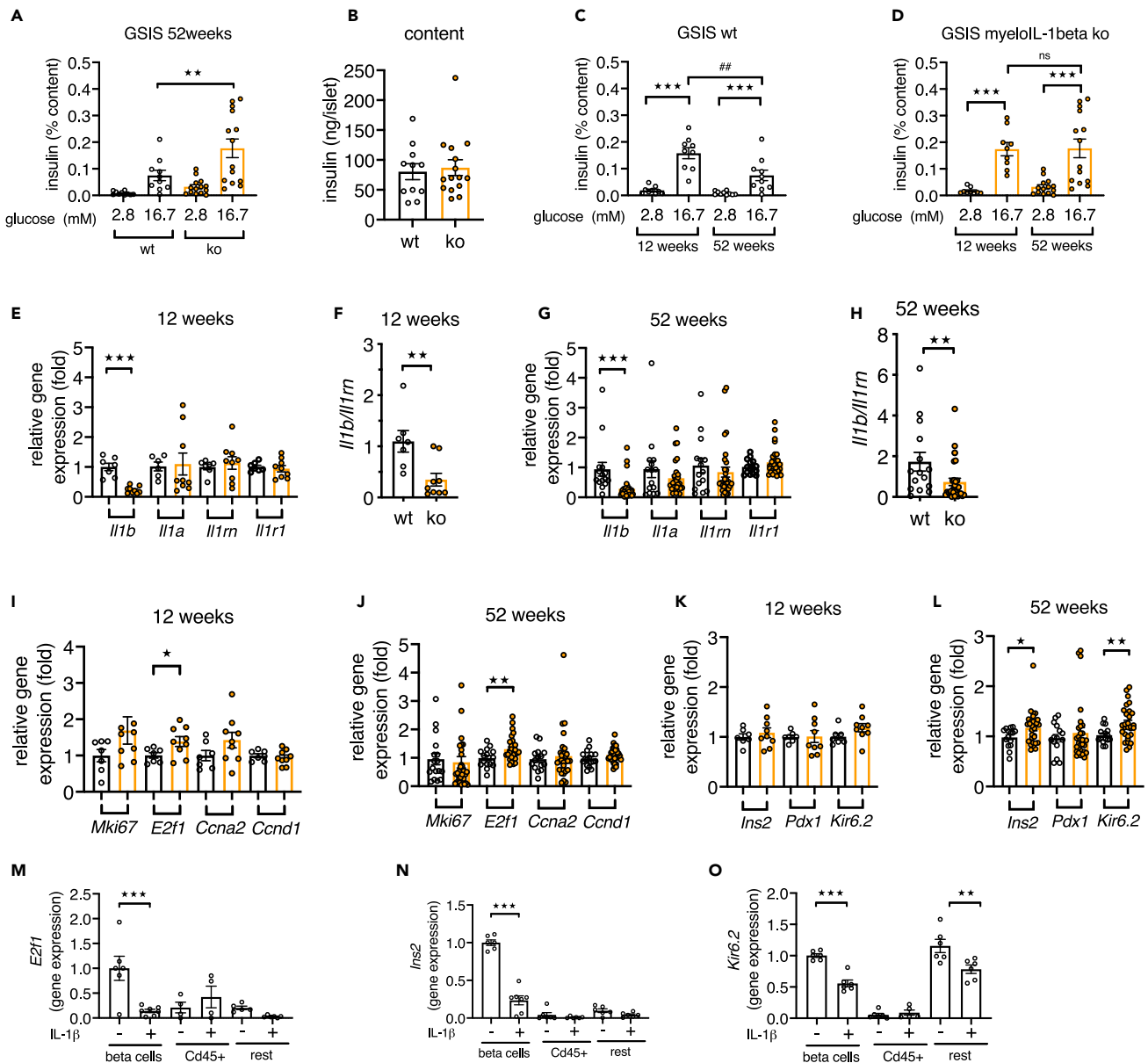
Figure 6. Deletion of IL-1beta in myeloid cells preserves insulin secretion in isolated islets from aged mice

(A and B) GSIS of isolated islets of 52-week-old myeloIL-1beta ko (orange) and littermate WT control (black) mice; (A) 1 h insulin secretion expressed as percentage of the insulin content per mouse; (B) insulin content per islet (mean of 3–4 x 10 islets per mouse; n = 10–11 WT and n = 14–15 ko mice).

(C and D) Comparison of GSIS data from Figure 6A with GSIS data from 12-week-old mice (mean of 3–4 ×10 islets per mouse, n = 9 WT and n = 9 ko mice).

(E, G, and I–L) Relative gene expression of islets from 12-week-old or 52-week-old myeloIL-1beta ko versus respective littermate controls.

(F and H) Ratio of *Il1b/Il1rn* gene expression. All data were expressed per mouse.

(M–O) Gene expression in FACS-isolated islet cell fractions from islets isolated from EYFP beta cell reporter mice and treated with or without 1 ng/ml IL-1beta (n = 4–7 FACS-isolated cell fractions from 4 separate experiments).

Statistics: (A, C, and D) two-way ANOVA and Sidak's multiple comparison test; (E–O) Student's t test; error bars represent SEM, *p < 0.05, **p < 0.01, ***p < 0.001, ##p < 0.01; ns, not significant. See also Figures S5A–S5E and S6.

data of islets from 52-week-old with those of 12-week-old mice (Figures S5C–S5E) showed that GSIS was decreased in islets from aged WT mice, whereas it did not decline in islets from myeloIL-1beta ko mice (Figures 6C and 6D). Unstimulated insulin secretion was similar in islets from myeloIL-1beta ko relative to their littermate controls (Figure 6A, p = 0.717 and Figure 6C p = 0.711). Taken together, islets from myeloIL-

1beta ko mice were protected from an age-associated decline of glucose-stimulated insulin secretion *in vivo* and *in vitro*. Next, we examined gene expression of islets from 12- and 52-weeks-old myeloIL-1beta ko and their respective littermate controls. *Il1b* gene expression was decreased by ca. 70% in islets from young and aged myeloIL-1beta ko mice relative to their respective WT controls, whereas islet *Il1a* or *Il1r1* gene expression was not different (Figures 6E–6H). In contrast to the whole-body IL-1beta ko mice, *Il1rn* expression was not upregulated in islets from aged myeloIL-1beta ko mice; however, the ratio of *Il1b/Il1rn* gene expression was also lower in these islets (Figures 6F and 6H), indicating diminished IL-1 activity. There was increased expression of *E2f1* in islets from 12- and 52-week-old myeloIL-1beta ko mice relative to their controls (Figures 6I and 6J), whereas *Ins2* and *Kir6.2* were increased in islets of aged myeloIL-1beta ko mice but not at 12-weeks of age (Figures 6K and 6L). Of note, in beta cells the cell-cycle regulator *E2f1* also regulates *Kir6.2* gene expression and thereby insulin secretion (Annicotte et al., 2009). Hence, the lack of IL-1beta in myeloid cells protected from age-related decline of genes encoding for factors important for insulin secretion. To examine whether *in vitro* treatment of islets with IL-1beta downregulated *Ins2*, *E2f1*, and *Kir6.2* expression in beta cells, we isolated islets from beta cell reporter mice and treated them with or without 1 ng/mL IL-1beta prior to FACS purification of EYFP + beta cells, CD45 + immune cells, and rest cells (qPCR of fraction marker controls; see Figure S6). Interestingly, *E2f1* had its highest expression in beta cells compared with the other islet cell fractions, and IL-1beta treatment reduced its expression in beta cells (Figure 6M). Similarly, IL-1beta downregulated *Ins2* in beta cells (Figure 6N) and *Kir6.2* in beta and in the rest cell fractions (Figure 6O). In addition, IL-1beta strongly induced chemokine *Cxcl1* expression in beta and rest cell fractions, whereas it induced *Il1a* and auto-induced itself in the CD45 + fraction (Figure S6). The *in vitro* suppression of *Ins2*, *E2f1*, and *Kir6.2* by IL-1beta in purified beta cells together with the differential expression of these genes in islets from aged myeloIL-1beta knockout mice suggested that myeloid-cell-derived IL-1beta directly downregulated *Ins2*, *E2f1*, and *Kir6.2* in beta cells *in vivo* during aging. Taken together, aged myeloIL-1beta ko mice had increased insulin secretion *in vivo* and *in vitro*; however, the phenotype was less pronounced than in whole-body IL-1beta ko mice.

DISCUSSION

In the present study, we describe a role of IL-1beta in the functional decline of beta cells during aging in mice. At 29 weeks of age, the expression of proliferation genes in whole islets was suppressed along with an increased ratio of *Il1b* to its protective antagonist *Il1rn*. Knockout of IL-1beta globally or specifically in myeloid cells protected pancreatic islets in aging and resulted in the common phenotype of elevated insulin secretion in 1-year-old mice. Aged IL-1beta ko mice additionally had increased beta cell mass. Isolated islets from both aged whole-body and myeloIL-1beta ko mice showed increased insulin secretion upon glucose stimulation, *Kir6.2* expression, and proliferation gene expression relative to littermate controls. This protection of beta cell function in aged IL-1beta knockout mice is in line with reported deleterious effects of IL-1beta treatments of islets *in vitro* (Bendtzen et al., 1986; Böni-Schnetzler and Meier, 2019; Maedler et al., 2002; Mandrup-Poulsen, 1996). This is also supported by results obtained in a mouse model with increased islet IL-1 signaling, in which beta-cell-specific *Il1rn* deletion resulted in diminished insulin secretion and smaller islets (Böni-Schnetzler et al., 2018).

Changes of expression of IL1 family genes in islets occurred early during the age trajectory (at 29 weeks). A comparison of FACS-purified islet cells from aged and young mice (isolated in parallel) showed that *Il1b* and *Il1rn* were selectively increased in CD45 + islet immune cells from aged mice. *Il1b* or *Il1a* gene expression were not detectable in FACS-isolated mouse beta and rest cell fractions, and upregulation of *Il1b* and *Il1a* expression by exogenous IL-1beta was only detectable in CD45 + immune cell fraction. Thereby, we conclude that in adult mouse islets *Il1a* and *Il1b* gene expression is confined to islet immune cells, as seen in reports where islet macrophages were depleted with chlodronate, which prevented *Il1b* expression in islets (Jourdan et al., 2013; Westwell-Roper et al., 2014). In contrast to these observations in mice, we detected low levels of *IL1B* gene expression in FACS-isolated human beta cells (Böni-Schnetzler et al., 2009). The analysis of FACS fractions of mouse islets further revealed that the age-associated cell-cycle gene inhibition mainly occurred in the beta and rest cell fractions and to a lesser extent in resident islet immune cells.

Although in humans there is a broad consensus that beta cell function declines with age, results in rodents are less clear-cut (Aguayo-Mazzucato, 2020). Many reports document an age-associated decrease in islets function in rodents (Aguayo-Mazzucato et al., 2017, 2019; Barker et al., 2015; Draznin et al., 1985; Krishnamurthy et al., 2006; Mihailidou et al., 2017; Molina et al., 1985; Reaven et al., 1983; Wang et al.,

1988; Westacott et al., 2017) or a preservation of function with age (Gregg et al., 2016; Tugay et al., 2016), whereas a few others reported an increase in glucose-stimulated insulin secretion with age (Avrahami et al., 2015; Wortham et al., 2018). However, these reports investigated maturation and compared juvenile and immature islets, which have a low glucose-stimulated insulin secretion, with aged mature islets. Of note, mature and immature beta cells coexist in islets of adult mice, whereby the proportion of cells with reduced maturity and insulin secretion increases during aging and T2D (Nasteska et al., 2021). We consistently observed in C57BL/6NCrl and various transgenic mouse lines that fasting insulin levels increased with age, whereas the glucose stimulation of insulin secretion decreased. In contrast, aged myeloIL-1beta ko mice also had increased fasting insulin levels relative to the levels at young age, yet they were still able to increase insulin secretion in response to a glucose bolus, indicating that IL-1beta knockout preserved beta cell function during aging. No age-related differences in insulin tolerance were observed in mye-loIL-1beta ko mice compared with littermate controls, suggesting that the improved insulin secretion of aged myeloIL-1beta ko mice was islet intrinsic. Indeed, isolated islets from aged myeloIL-1beta ko mice also had preserved secretory function, whereas it declined in islets from aged control mice.

The insulin secretion phenotype was much more pronounced in aged global IL-1beta ko than in myeloIL-1beta ko mice, which may have several reasons. Firstly, myeloIL-1beta ko mice had partial *Il1b* depletion (approximately 70%) in their islets, whereas *Il1b* was absent in whole-body IL-1beta ko mice along with a reduction of *Il1a* expression. Secondly, the size and number of islets were increased in IL-1beta ko mice relative to aged littermates, whereas aged myeloIL-1beta ko mice had increased glucose-stimulated insulin secretion without an apparent increase of beta cell mass. Lastly, insulin secretion and beta cell mass expansion in aged IL-1beta ko mice could have been further amplified by insulin resistance observed in 52-week-old IL-1beta ko mice. Following a period of unchanged insulin tolerance and insulin secretion in younger 24-week-old IL-1beta ko mice, both increased insulin secretion and insulin resistance appeared at 52 weeks of age relative to controls. Thus, from these data alone it cannot be concluded whether increased insulin secretion or insulin resistance are the primary phenotype. However, because aged myeloIL-1beta ko mice at 52 weeks also showed increased glucose-induced insulin secretion but not insulin resistance or impaired glucose tolerance at any age, it is likely that the elevated insulin secretion in IL-1beta ko mice was an early phenotype that may have promoted insulin resistance. Indeed, transgenic hyperinsulinemia in mice or basal hyperinsulinemia due to insulinomas in humans also leads to insulin resistance (Shanik et al., 2008).

Consistent with higher insulin secretion, aged whole-body IL-1beta and myeloIL-1beta ko mice had elevated expression of genes associated with insulin secretion and cell-cycle control compared with their littermates. IL-1beta ko mice had higher *Mki67* gene expression, and myeloIL-1beta ko mice had higher *E21f and Ins2* expression. Interestingly, in beta cells the transcription factor *E2f1* not only controls cell cycle but also regulates insulin secretion (Annicotte et al., 2009; Grouwels et al., 2010). Moreover, ectopic *E2f1* expression rescued reduced GSIS in islets from mice with beta-cell-specific IL-1Ra knockout, an *in vivo* model for chronic unopposed IL-1 signaling in islets (Böni-Schnetzler et al., 2018). Both IL-1beta ko models had increased *Kir6.2* expression in islets from aged mice. Recent RNAseq coupled with electrophysiology uncovered that the dysfunctional beta cell phenotype in human T2D was related to cell-cycle pathways and that IL1 signaling was negatively correlated with insulin exocytosis (Camunas-Soler et al., 2020). In GWAS with human T2D, Kir6.2 (*KCNJ11*) is one of the top associated genes (Florez et al., 2004; Gloyn et al., 2003; Saxena et al., 2007), and its expression declines with age (Kirkpatrick et al., 2010). In several preclinical studies with animal models of T2D and in clinical studies with human T2D, inhibition of IL-1 led to improved insulin secretion (Donath et al., 2019; Ehses et al., 2009; Larsen et al., 2007; Owyang et al., 2010; Sauter et al., 2008). Because IL-1beta ko resulted in preserved beta cell function in aged mice, one could hypothesize that part of the observed clinical benefit of IL-1 antagonism in patients with T2D may come from an amelioration of the age-related decline of beta cells.

A deleterious role of IL-1beta on insulin secretion was previously described in the context of low-grade inflammation in metabolic diseases including obesity and T2D (Donath and Shoelson, 2011; Gregor and Hotamisligil, 2011; Herder et al., 2015). Here we propose that chronic IL-1beta exposure to islets during aging decreases glucose-stimulated insulin secretion. Indeed, islet macrophages, which are a major source of IL-1beta in islets (Jourdan et al., 2013; Westwell-Roper et al., 2014), have high levels of IL-1beta expression relative to other resident tissue macrophages (Brykczynska et al., 2020). In addition, we show that expression levels of IL-1beta further increase with age in islet immune cells (Figure 2G), which may sustain

a chronic state of IL-1 action on islets. Supporting this notion, recent secretome analysis of senescent mouse and human beta cells revealed an enrichment in IL-1 signaling pathways (Midha et al., 2021).

More recently, a physiological role of IL-1beta on insulin secretion has emerged during fasting-refeeding, endotoxin treatment, adaptation to short-term high-fat diet feeding (Dror et al., 2017; Hajmrle et al., 2016), and in mouse models with constitutive pancreatic deletion of the IL-1R1 or IL-1alpha (Burke et al., 2018; Collier et al., 2021). At first glance this beneficial and adaptive role of IL-1beta appears to be at odds with the deleterious chronic effects of IL-1beta on insulin secretion. A possible explanation to reconcile these opposing IL-1beta effects on beta cell function is the consequence of acute versus chronic stimulation of insulin secretion. Chronic stimulation may exhaust beta cells or induce resistance to IL-1beta stimulation (Hajmrle et al., 2016). Furthermore, over time, there may be changes in transcriptional programs, which regulate insulin secretion and beta cell turnover, and because the rate of beta cell turnover is very low, it may gradually take time for deleterious effects on beta cell mass to manifest. Moreover, there may be changes over time in IL-1 counter-regulation. Indeed, we observed here an age-associated decrease of expression of the protective *Il1rn* in *ex vivo* isolated islets.

The beneficial role of IL-1beta on insulin secretion was mostly observed in acute and short-term exposure (single injection of IL-1beta or LPS, fasting-refeeding, or 4-day high-fat diet feeding) *in vivo* as well as *in vitro* (Spinas et al., 1988). Recently, deleterious long-term effects (in 9-months-old male mice) on glucose tolerance in mice with pancreatic deletion of either the IL-1R1 or IL-1alpha (Burke et al., 2018; Collier et al., 2021) were reported, and it was concluded that IL-1R1 signaling and IL-1alpha are needed for proper metabolic control in older mice. Because a constitutive Pdx-Cre driver mouse line that targets the whole pancreas, entero-endocrine cells, and the hypothalamus was used for knockout induction, it is possible that there is a role for IL-1R1 and IL-1alpha in the development of these tissues, which only manifests later in life. Indeed, macrophages, which are the main source of IL-1 agonists, are required for proper pancreas development (Banaei-Bouchareb et al., 2004). Because we saw no deterioration of glucose tolerance in whole-body and myeloIL-1beta ko mice at young and old age, and because IL-1alpha and IL-1beta engage the same receptor, one could alternatively speculate that the long-term beneficial role these authors saw in their mouse models is selective for IL-1alpha signaling. Noteworthy, we were unable to detect IL-1alpha in purified islet beta cells, indicating that these beneficial effects may stem from other tissues targeted by Pdx-Cre. Thus, beta-cell-specific and inducible Cre driver models together with indispensable age-matched Cre-only controls (Magnuson and Osipovich, 2013) would be needed to further shed light on these questions.

In conclusion, we showed increased IL1 family gene expression in islet immune cells, whereas the protective *Il1rn* declined in islets during aging. Lack of IL-1beta globally or in myeloid cells protected islets from an age-associated decline of beta cell function by differential expression of genes involved in the regulation of insulin secretion and cell-cycle control. We propose that long-term chronic IL-1beta signaling in islets promotes the age-associated deterioration of beta cell function.

Limitations of study

A limitation of the study is the use of global germline IL-1beta knockouts, which may cause early developmental effects. However, the main phenotype, preserved insulin secretion during aging, was also observed in myeloIL-1beta ko mice, where IL-1beta was only partially depleted. Moreover, the whole-body IL-1beta ko mice have no Cre recombinase expression that could cause a phenotype by Cre itself as previously reported for many pancreatic Cre driver lines (Magnuson and Osipovich, 2013). Further, we performed control experiments, with aged *Lyz2* Cre-only mice showing that the effects observed in myeloIL-1beta ko mice was not influenced by Cre expression and we always used littermate control mice. Moreover, mice were on a pure genetic background that do not harbor the Nnt gene deletion influencing insulin secretion as seen in C57BL/6J mice (Attane et al., 2016; Freeman et al., 2006).

A general limitation of aging experiments is the variability in body weight of age-matched mice that increases with age. To account for this, we used a large number of aged mice to assess their *in vivo* phenotype and to measure beta cell function and gene expression in isolated islets. Compared with other mouse tissues, beta cells have one of the highest *Il1r1* expression levels (Benner et al., 2014; Böni-Schnetzler et al., 2009), strongly suggesting that chronic IL-1beta directly acts on beta cells during aging. However, it is also

possible that IL-1beta indirectly impairs beta cells through IL-1beta-induced chemokines and age-associated increase of T cells (Denroche et al., 2021).

STAR★METHODS

Detailed methods are provided in the online version of this paper and include the following:

- KEY RESOURCES TABLE
- RESOURCE AVAILABILITY
  - Lead contact
  - Materials availability
  - Data and code availability
- EXPERIMENTAL MODEL AND SUBJECT DETAILS
  - Experimental animals
  - Animal husbandary
- METHOD DETAILS
  - Glucose and insulin tolerance tests
  - Mouse islet isolation
  - Isolation of islet beta and immune cells from 12- and 52-week-old mice by FACS
  - Treatment of isolated islets with IL-1beta
  - Isolation of peritoneal cells to determine IL-1beta protein release
  - Glucose-stimulated insulin secretion assay of isolated islets
  - Hormone and cytokine detection
  - Determination of beta cell mass and islet area from IL-1beta ko and myeloIL-1beta ko mice and respective littermate controls
  - Determination of Ki67 + beta cells in histology sections from IL-1beta ko and littermate control mice
  - RNA extraction and qPCR
- QUANTIFICATION AND STATISTICAL ANALYSIS

SUPPLEMENTAL INFORMATION

Supplemental information can be found online at https://doi.org/10.1016/j.isci.2021.103250.

AUTHOR CONTRIBUTIONS

Conceptualization, M.B.-S. and M.Y.D.; Methodology, M.B.-S., D.T.M.; Formal analysis, M.B.-S.; Investigation, M.B.-S, H.M., L.R., S.J.W., K.T., F.S., D.T.M.; Writing-Original Draft, M.B.-S.; Writing-Review and Editing, M.B.-S., M.Y.D., D.T.M.; Funding Acquisition, M.Y.D.

DECLARATION OF INTERESTS

M.Y.D. is listed as the inventor on a patent filed in 2003 for the use of an IL-1 receptor antagonist for the treatment of or prophylaxis for type 2 diabetes.

REFERENCES

Aguayo-Mazzucato, C. (2020). Functional changes in beta cells during ageing and senescence. Diabetologia 63, 2022–2029.

Aguayo-Mazzucato, C., Andle, J., Lee, T.B., Jr., Midha, A., Talemal, L., Chipashvili, V., Hollister-Lock, J., van Deursen, J., Weir, G., and Bonner-Weir, S. (2019). Acceleration of beta cell aging determines diabetes and senolysis improves disease outcomes. Cell Metab. 30, 129–142 e124.

Aguayo-Mazzucato, C., van Haaren, M., Mruk, M., Lee, T.B., Jr., Crawford, C., Hollister-Lock, J., Sullivan, B.A., Johnson, J.W., Ebrahimi, A., Dreyfuss, J.M., et al. (2017). Beta cell aging markers have heterogeneous distribution and are induced by insulin resistance. Cell Metab. 25, 898–910 e895.

Almaca, J., Molina, J., Arrojo, E.D.R., Abdulreda, M.H., Jeon, W.B., Berggren, P.O., Caicedo, A., and Nam, H.G. (2014). Young capillary vessels rejuvenate aged pancreatic islets. Proc. Natl. Acad. Sci. U S A 111, 17612–17617.

Annicotte, J.S., Blanchet, E., Chavey, C., Iankova, I., Costes, S., Assou, S., Teyssier, J., Dalle, S., Sardet, C., and Fajas, L. (2009). The CDK4-pRB-E2F1 pathway controls insulin secretion. Nat. Cell Biol. 11, 1017–1023.

Attane, C., Peyot, M.L., Lussier, R., Zhang, D., Joly, E., Madiraju, S.R., and Prentki, M. (2016). Differential insulin secretion of high-fat diet-fed C57bl/6NN and C57bl/6NJ mice: implications of mixed genetic background in metabolic studies. PLoS One 11, e0159165.

Avrahami, D., Li, C., Zhang, J., Schug, J., Avrahami, R., Rao, S., Stadler, M.B., Burger, L., Schubeler, D., Glaser, B., et al. (2015). Aging-Dependent demethylation of regulatory elements correlates with chromatin state and improved beta cell function. Cell Metab. 22, 619–632.

Banaei-Bouchareb, L., Gouon-Evans, V., Samara-Boustani, D., Castellotti, M.C., Czernichow, P., Pollard, J.W., and Polak, M. (2004). Insulin cell mass is altered in Csf1op/Csf1op macrophage-deficient mice. J. Leukoc. Biol. 76, 359–367.

Barker, C.J., Li, L., Kohler, M., and Berggren, P.O. (2015). beta-Cell Ca(2+) dynamics and function are compromised in aging. Adv. Biol. Regul. 57, 112–119.

Barzilai, N., Huffman, D.M., Muzumdar, R.H., and Bartke, A. (2012). The critical role of metabolic pathways in aging. Diabetes 61, 1315–1322.

Basu, R., Breda, E., Oberg, A.L., Powell, C.C., Dalla Man, C., Basu, A., Vittone, J.L., Klee, G.G., Arora, P., Jensen, M.D., et al. (2003). Mechanisms of the age-associated deterioration in glucose tolerance: contribution of alterations in insulin secretion, action, and clearance. Diabetes 52, 1738–1748.

Bendtzen, K., Mandrup-Poulsen, T., Nerup, J., Nielsen, J.H., Dinarello, C.A., and Svenson, M. (1986). Cytotoxicity of human pI 7 interleukin-1 for pancreatic islets of Langerhans. Science 232, 1545–1547.

Benner, C., van der Meulen, T., Caceres, E., Tigyi, K., Donaldson, C.J., and Huising, M.O. (2014). The transcriptional landscape of mouse beta cells compared to human beta cells reveals notable species differences in long non-coding RNA and protein-coding gene expression. BMC Genomics 15, 620.

Berg, S., Kutra, D., Kroeger, T., Straehle, C.N., Kausler, B.X., Haubold, C., Schiegg, M., Ales, J., Beier, T., Rudy, M., et al. (2019). ilastik: interactive machine learning for (bio)image analysis. Nat. Methods 16, 1226–1232.

Böni-Schnetzler, M., Boller, S., Debray, S., Bouzakri, K., Meier, D.T., Prazak, R., Kerr-Conte, J., Pattou, F., Ehses, J.A., Schuit, F.C., et al. (2009). Free fatty acids induce a proinflammatory response in islets via the abundantly expressed interleukin-1 receptor I. Endocrinology 150, 5218–5229.

Böni-Schnetzler, M., Hauselmann, S.P., Dalmas, E., Meier, D.T., Thienel, C., Traub, S., Schulze, F., Steiger, L., Dror, E., Martin, P., et al. (2018). Beta cell-specific deletion of the IL-1 receptor antagonist impairs beta cell proliferation and insulin secretion. Cell Rep. 22, 1774–1786.

Böni-Schnetzler, M., and Meier, D.T. (2019). Islet inflammation in type 2 diabetes. Semin. Immunopathol. 41, 501–513.

Brykczynska, U., Geigges, M., Wiedemann, S.J., Dror, E., Böni-Schnetzler, M., Hess, C., Donath, M.Y., and Paro, R. (2020). Distinct transcriptional responses across tissue-resident macrophages to short-term and long-term metabolic challenge. Cell Rep. 30, 1627–1643 e1627.

Burke, S.J., Batdorf, H.M., Burk, D.H., Martin, T.M., Mendoza, T., Stadler, K., Alami, W., Karlstad, M.D., Robson, M.J., Blakely, R.D., et al. (2018). Pancreatic deletion of the interleukin-1 receptor disrupts whole body glucose homeostasis and promotes islet beta-cell de-differentiation. Mol. Metab. 14, 95–107.

Calderon, B., Carrero, J.A., Ferris, S.T., Sojka, D.K., Moore, L., Epelman, S., Murphy, K.M., Yokoyama, W.M., Randolph, G.J., and Unanue, E.R. (2015). The pancreas anatomy conditions the origin and properties of resident macrophages. J. Exp. Med. 212, 1497–1512.

Camunas-Soler, J., Dai, X.Q., Hang, Y., Bautista, A., Lyon, J., Suzuki, K., Kim, S.K., Quake, S.R., and MacDonald, P.E. (2020). Patch-seq links single-cell transcriptomes to human islet dysfunction in diabetes. Cell Metab. 31, 1017–1031 e1014.

Chia, C.W., Egan, J.M., and Ferrucci, L. (2018). Age-related changes in glucose metabolism, hyperglycemia, and cardiovascular risk. Circ. Res. 123, 886–904.

Clausen, B.E., Burkhardt, C., Reith, W., Renkawitz, R., and Forster, I. (1999). Conditional gene targeting in macrophages and granulocytes using LysMcre mice. Transgenic Res. 8, 265–277.

Collier, J.J., Batdorf, H.M., Martin, T.M., Rohli, K.E., Burk, D.H., Lu, D., Cooley, C.R., Karlstad, M.D., Jackson, J.W., Sparer, T.E., et al. (2021). Pancreatic, but not myeloid-cell, expression of interleukin-1alpha is required for maintenance of insulin secretion and whole body glucose homeostasis. Mol. Metab. 44, 101140.

Cree, L.M., Patel, S.K., Pyle, A., Lynn, S., Turnbull, D.M., Chinnery, P.F., and Walker, M. (2008). Age-related decline in mitochondrial DNA copy number in isolated human pancreatic islets. Diabetologia 51, 1440–1443.

Dalmas, E., Lehmann, F.M., Dror, E., Wueest, S., Thienel, C., Borsigova, M., Stawiski, M., Traunecker, E., Lucchini, F.C., Dapito, D.H., et al. (2017). Interleukin-33-Activated islet-resident innate lymphoid cells promote insulin secretion through myeloid cell retinoic acid production. Immunity 47, 928–942 e927.

De Tata, V. (2014). Age-related impairment of pancreatic Beta-cell function: pathophysiological and cellular mechanisms. Front. Endocrinol. 5, 138.

DeFronzo, R.A. (1981). Glucose intolerance and aging. Diabetes Care 4, 493–501.

Denroche, H.C., Miard, S., Salle-Lefort, S., Picard, F., and Verchere, C.B. (2021). T cells accumulate in non-diabetic islets during ageing. Immun. Ageing 18, 8.

Donath, M.Y., Meier, D.T., and Böni-Schnetzler, M. (2019). Inflammation in the pathophysiology and therapy of cardiometabolic disease. Endocr. Rev. 40, 1080–1091.

Donath, M.Y., and Shoelson, S.E. (2011). Type 2 diabetes as an inflammatory disease. Nat. Rev. Immunol. 11, 98–107.

Draznin, B., Steinberg, J.P., Leitner, J.W., and Sussman, K.E. (1985). The nature of insulin secretory defect in aging rats. Diabetes 34, 1168–1173.

Dror, E., Dalmas, E., Meier, D.T., Wueest, S., Thevenet, J., Thienel, C., Timper, K., Nordmann, T.M., Traub, S., Schulze, F., et al. (2017). Postprandial macrophage-derived IL-1beta stimulates insulin, and both synergistically promote glucose disposal and inflammation. Nat. Immunol. 18, 283–292.

Eguchi, K., Manabe, I., Oishi-Tanaka, Y., Ohsugi, M., Kono, N., Ogata, F., Yagi, N., Ohto, U., Kimoto, M., Miyake, K., et al. (2012). Saturated fatty acid and TLR signaling link beta cell dysfunction and islet inflammation. Cell Metab. 15, 518–533.

Ehses, J.A., Lacraz, G., Giroix, M.H., Schmidlin, F., Coulaud, J., Kassis, N., Irminger, J.C., Kergoat, M., Portha, B., Homo-Delarche, F., et al. (2009). IL-1 antagonism reduces hyperglycemia and tissue inflammation in the type 2 diabetic GK rat. Proc. Natl. Acad. Sci. U S A 106, 13998–14003.

Ferris, S.T., Zakharov, P.N., Wan, X., Calderon, B., Artyomov, M.N., Unanue, E.R., and Carrero, J.A. (2017). The islet-resident macrophage is in an inflammatory state and senses microbial products in blood. J. Exp. Med. 214, 2369–2385.

Florez, J.C., Burtt, N., de Bakker, P.I., Almgren, P., Tuomi, T., Holmkvist, J., Gaudet, D., Hudson, T.J., Schaffner, S.F., Daly, M.J., et al. (2004). Haplotype structure and genotype-phenotype correlations of the sulfonylurea receptor and the islet ATP-sensitive potassium channel gene region. Diabetes 53, 1360–1368.

Freeman, H.C., Hugill, A., Dear, N.T., Ashcroft, F.M., and Cox, R.D. (2006). Deletion of nicotinamide nucleotide transhydrogenase: a new quantitive trait locus accounting for glucose intolerance in C57BL/6J mice. Diabetes 55, 2153–2156.

Gloyn, A.L., Weedon, M.N., Owen, K.R., Turner, M.J., Knight, B.A., Hitman, G., Walker, M., Levy, J.C., Sampson, M., Halford, S., et al. (2003). Large-scale association studies of variants in genes encoding the pancreatic beta-cell KATP channel subunits Kir6.2 (KCNJ11) and SUR1 (ABCC8) confirm that the KCNJ11 E23K variant is associated with type 2 diabetes. Diabetes 52, 568–572.

Gregg, T., Poudel, C., Schmidt, B.A., Dhillon, R.S., Sdao, S.M., Truchan, N.A., Baar, E.L., Fernandez, L.A., Denu, J.M., Eliceiri, K.W., et al. (2016). Pancreatic beta-cells from mice offset age-associated mitochondrial deficiency with reduced KATP channel activity. Diabetes 65, 2700–2710.

Gregor, M.F., and Hotamisligil, G.S. (2011). Inflammatory mechanisms in obesity. Annu. Rev. Immunol. 29, 415–445.

Grouwels, G., Cai, Y., Hoebeke, I., Leuckx, G., Heremans, Y., Ziebold, U., Stange, G., Chintinne, M., Ling, Z., Pipeleers, D., et al. (2010). Ectopic expression of E2F1 stimulates beta-cell proliferation and function. Diabetes 59, 1435–1444.

Gumbiner, B., Polonsky, K.S., Beltz, W.F., Wallace, P., Brechtel, G., and Fink, R.I. (1989). Effects of aging on insulin secretion. Diabetes 38, 1549–1556.

Guo, N., Parry, E.M., Li, L.S., Kembou, F., Lauder, N., Hussain, M.A., Berggren, P.O., and Armanios, M. (2011). Short telomeres compromise beta-cell signaling and survival. PLoS One 6, e17858.

Hajmrle, C., Smith, N., Spigelman, A.F., Dai, X., Senior, L., Bautista, A., Ferdaoussi, M., and MacDonald, P.E. (2016). Interleukin-1 signaling contributes to acute islet compensation. JCI Insight 1, e86055.

Helman, A., Klochendler, A., Azazmeh, N., Gabai, Y., Horwitz, E., Anzi, S., Swisa, A., Condiotti, R., Granit, R.Z., Nevo, Y., et al. (2016). p16(Ink4a)-induced senescence of pancreatic beta cells enhances insulin secretion. Nat. Med. 22, 412–420.

Herder, C., Dalmas, E., Böni-Schnetzler, M., and Donath, M.Y. (2015). The IL-1 pathway in type 2 diabetes and cardiovascular complications. Trends Endocrinol. Metab. 26, 551–563.

Herrera, P.L., Nepote, V., and Delacour, A. (2002). Pancreatic cell lineage analyses in mice. Endocrine 19, 267–278.

Ihm, S.H., Moon, H.J., Kang, J.G., Park, C.Y., Oh, K.W., Jeong, I.K., Oh, Y.S., and Park, S.W. (2007). Effect of aging on insulin secretory function and expression of beta cell function-related genes of islets. Diabetes Res. Clin. Pract. 77, S150–S154.

Iozzo, P., Beck-Nielsen, H., Laakso, M., Smith, U., Yki-Jarvinen, H., and Ferrannini, E. (1999). Independent influence of age on basal insulin secretion in nondiabetic humans. European Group for the Study of Insulin Resistance. J. Clin. Endocrinol. Metab. 84, 863–868.

Janjuha, S., Singh, S.P., Tsakmaki, A., Mousavy Gharavy, S.N., Murawala, P., Konantz, J., Birke, S., Hodson, D.J., Rutter, G.A., Bewick, G.A., et al. (2018). Age-related islet inflammation marks the proliferative decline of pancreatic beta-cells in zebrafish. Elife 7, e32965.

Jourdan, T., Godlewski, G., Cinar, R., Bertola, A., Szanda, G., Liu, J., Tam, J., Han, T., Mukhopadhyay, B., Skarulis, M.C., et al. (2013). Activation of the Nlrp3 inflammasome in infiltrating macrophages by endocannabinoids mediates beta cell loss in type 2 diabetes. Nat. Med. 19, 1132–1140.

Kirkpatrick, C.L., Marchetti, P., Purrello, F., Piro, S., Bugliani, M., Bosco, D., de Koning, E.J., Engelse, M.A., Kerr-Conte, J., Pattou, F., et al. (2010). Type 2 diabetes susceptibility gene expression in normal or diabetic sorted human alpha and beta cells: correlations with age or BMI of islet donors. PLoS One 5, e11053.

Krishnamurthy, J., Ramsey, M.R., Ligon, K.L., Torrice, C., Koh, A., Bonner-Weir, S., and Sharpless, N.E. (2006). p16INK4a induces an age-dependent decline in islet regenerative potential. Nature 443, 453–457.

Larsen, C.M., Faulenbach, M., Vaag, A., Volund, A., Ehses, J.A., Seifert, B., Mandrup-Poulsen, T., and Donath, M.Y. (2007). Interleukin-1-receptor antagonist in type 2 diabetes mellitus. N. Engl. J. Med. 356, 1517–1526.

Lopez-Otin, C., Blasco, M.A., Partridge, L., Serrano, M., and Kroemer, G. (2013). The hallmarks of aging. Cell 153, 1194–1217.

Maedler, K., Sergeev, P., Ris, F., Oberholzer, J., Joller-Jemelka, H.I., Spinas, G.A., Kaiser, N., Halban, P.A., and Donath, M.Y. (2002). Glucose-induced beta-cell production of interleukin-1beta contributes to glucotoxicity in human pancreatic islets. J. Clin. Invest. 110, 851–860.

Magnuson, M.A., and Osipovich, A.B. (2013). Pancreas-specific Cre driver lines and considerations for their prudent use. Cell Metab. 18, 9–20.

Mandrup-Poulsen, T. (1996). The role of interleukin-1 in the pathogenesis of IDDM. Diabetologia 39, 1005–1029.

Meier, J.J., Butler, A.E., Saisho, Y., Monchamp, T., Galasso, R., Bhushan, A., Rizza, R.A., and Butler, P.C. (2008). Beta-cell replication is the primary mechanism subserving the postnatal expansion of beta-cell mass in humans. Diabetes 57, 1584–1594.

Meneilly, G.S., Veldhuis, J.D., and Elahi, D. (1999). Disruption of the pulsatile and entropic modes of insulin release during an unvarying glucose stimulus in elderly individuals. J. Clin. Endocrinol. Metab. 84, 1938–1943.

Midha, A., Pan, H., Abarca, C., Andle, J., Carapeto, P., Bonner-Weir, S., and Aguayo-Mazzucato, C. (2021). Unique human and mouse beta-cell senescence-associated secretory phenotype (SASP) reveal conserved signaling pathways and heterogeneous factors. Diabetes 70, 1098–1116.

Mihailidou, C., Chatzistamou, I., Papavassiliou, A.G., and Kiaris, H. (2017). Modulation of pancreatic islets' function and survival during aging involves the differential regulation of endoplasmic reticulum stress by p21 and CHOP. Antioxid. Redox Signal. 27, 185–200.

Molina, J.M., Premdas, F.H., and Lipson, L.G. (1985). Insulin release in aging: dynamic response of isolated islets of Langerhans of the rat to D-glucose and D-glyceraldehyde. Endocrinology 116, 821–826.

Munoz-Espin, D., and Serrano, M. (2014). Cellular senescence: from physiology to pathology. Nat. Rev. Mol. Cell Biol. 15, 482–496.

Nasteska, D., Fine, N.H.F., Ashford, F.B., Cuozzo, F., Viloria, K., Smith, G., Dahir, A., Dawson, P.W.J., Lai, Y.C., Bastidas-Ponce, A., et al. (2021). PDX1(LOW) MAFA(LOW) beta-cells contribute to islet function and insulin release. Nat. Commun. 12, 674.

Novelli, M., De Tata, V., Bombara, M., Bergamini, E., and Masiello, P. (2000). Age-dependent reduction in GLUT-2 levels is correlated with the impairment of the insulin secretory response in isolated islets of Sprague-Dawley rats. Exp. Gerontol. 35, 641–651.

Owyang, A.M., Maedler, K., Gross, L., Yin, J., Esposito, L., Shu, L., Jadhav, J., Domsgen, E., Bergemann, J., Lee, S., et al. (2010). XOMA 052, an anti-IL-1{beta} monoclonal antibody, improves glucose control and {beta}-cell function in the diet-induced obesity mouse model. Endocrinology 151, 2515–2527.

Reaven, E., Wright, D., Mondon, C.E., Solomon, R., Ho, H., and Reaven, G.M. (1983). Effect of age and diet on insulin secretion and insulin action in the rat. Diabetes 32, 175–180.

Ribeiro, R.A., Batista, T.M., Coelho, F.M., Boschero, A.C., Lopes, G.S., and Carneiro, E.M. (2012). Decreased beta-cell insulin secretory function in aged rats due to impaired Ca(2+) handling. Exp. Physiol. 97, 1065–1073.

Sauter, N.S., Schulthess, F.T., Galasso, R., Castellani, L.W., and Maedler, K. (2008). The antiinflammatory cytokine interleukin-1 receptor antagonist protects from high-fat diet-induced hyperglycemia. Endocrinology 149, 2208–2218.

Saxena, R., Voight, B.F., Lyssenko, V., Burtt, N.P., de Bakker, P.I., Chen, H., Roix, J.J., Kathiresan, S., Hirschhorn, J.N., Daly, M.J., et al. (2007). Genome-wide association analysis identifies loci for type 2 diabetes and triglyceride levels. Science 316, 1331–1336.

Schindelin, J., Arganda-Carreras, I., Frise, E., Kaynig, V., Longair, M., Pietzsch, T., Preibisch, S., Rueden, C., Saalfeld, S., Schmid, B., et al. (2012). Fiji: an open-source platform for biological-image analysis. Nat. Methods 9, 676–682.

Schmittgen, T.D., and Livak, K.J. (2008). Analyzing real-time PCR data by the comparative C(T) method. Nat. Protoc. 3, 1101–1108.

Shanik, M.H., Xu, Y., Skrha, J., Dankner, R., Zick, Y., and Roth, J. (2008). Insulin resistance and hyperinsulinemia: is hyperinsulinemia the cart or the horse? Diabetes Care 31, S262–S268.

Spinas, G.A., Palmer, J.P., Mandrup-Poulsen, T., Andersen, H., Nielsen, J.H., and Nerup, J. (1988). The bimodal effect of interleukin 1 on rat pancreatic beta-cells– stimulation followed by inhibition–depends upon dose, duration of exposure, and ambient glucose concentration. Acta Endocrinol. *119*, 307–311.

Srinivas, S., Watanabe, T., Lin, C.S., William, C.M., Tanabe, Y., Jessell, T.M., and Costantini, F. (2001). Cre reporter strains produced by targeted insertion of EYFP and ECFP into the ROSA26 locus. BMC Dev. Biol. *1*, 4.

Teta, M., Long, S.Y., Wartschow, L.M., Rankin, M.M., and Kushner, J.A. (2005). Very slow turnover of beta-cells in aged adult mice. Diabetes *54*, 2557–2567.

Tschen, S.I., Dhawan, S., Gurlo, T., and Bhushan, A. (2009). Age-dependent decline in beta-cell proliferation restricts the capacity of beta-cell regeneration in mice. Diabetes *58*, 1312–1320.

Tugay, K., Guay, C., Marques, A.C., Allagnat, F., Locke, J.M., Harries, L.W., Rutter, G.A., and Regazzi, R. (2016). Role of microRNAs in the age-associated decline of pancreatic beta cell function in rat islets. Diabetologia *59*, 161–169.

Wang, S.Y., Halban, P.A., and Rowe, J.W. (1988). Effects of aging on insulin synthesis and secretion. Differential effects on preproinsulin messenger RNA levels, proinsulin biosynthesis, and secretion of newly made and preformed insulin in the rat. J. Clin. Invest *81*, 176–184.

Westacott, M.J., Farnsworth, N.L., St Clair, J.R., Poffenberger, G., Heintz, A., Ludin, N.W., Hart, N.J., Powers, A.C., and Benninger, R.K.P. (2017). Age-Dependent decline in the coordinated [Ca(2+)] and insulin secretory dynamics in human pancreatic islets. Diabetes *66*, 2436–2445.

Westwell-Roper, C.Y., Ehses, J.A., and Verchere, C.B. (2014). Resident macrophages mediate islet amyloid polypeptide-induced islet IL-1beta production and beta-cell dysfunction. Diabetes *63*, 1698–1711.

Wortham, M., Benthuysen, J.R., Wallace, M., Savas, J.N., Mulas, F., Divakaruni, A.S., Liu, F., Albert, V., Taylor, B.L., Sui, Y., et al. (2018). Integrated in vivo quantitative proteomics and Nutrient tracing reveals age-related metabolic rewiring of pancreatic beta cell function. Cell Rep. *25*, 2904–2918 e2908.

STAR★METHODS

KEY RESOURCES TABLE

REAGENT or RESOURCE	SOURCE	IDENTIFIER
Antibodies		
anti-Mouse CD16/CD32 (clone17A34)	BioLegend	Cat#158302; RRID: AB_2876546
APC anti-mouse CD45 (clone 30-F11)	eBioscience	Cat#17-0451-83; RRID: AB_469392
Guinea pig anti-insulin (polyclonal)	Dako	Cat#A0564; RRID: AB_10013624
Rat anti-mouse CD45 (30-F11)	BD Pharmingen	Cat#550539; RRID: AB_2174426
Alexa Fluor 647-conjugated goat anti–Guinea pig IgG	Fischer Scientific	Cat#A-21450; RRID: AB_2735091
Alexa Fluor 555-conjugated goat anti-rat IgG	Fischer Scientific	Cat#A21434; RRID: AB_2535855
Ki-67 monoclonal antibody (SolA15), Biotin	eBioscience™	Cat#13-5698-82; RRID: AB_11151153
Fluorescein (FITC) AffiniPure F(ab')₂ Fragment Donkey Anti-Guinea pig IgG (H + L)	JacksonImmunoResearch	Cat#706-096-148; RRID:AB_2340454
Chemicals, peptides, and recombinant proteins		
Recombinant mouse IL-1beta	Bio-Techne, Switzerland	Cat# MRA00
Trypsin	GIBCO	Cat# 154,000-054
LPS from S. Minnesota R595	InvivoGen	Cat# tlrl-smlps
Collagenase type 4	Worthington	Cat# CLS-4
ATP	InvivoGen	Cat# tlrl-atp
DNA-binding dye DAPI	SIGMA	10,236,276,001
0.5% Trypsin-EDTA (x10)	Thermo Fisher Scientific	Cat# 15,400,054
Insulin	Novo Nordisk	Actrapid^R HM
Critical commercial assays		
V-plex mouse IL-1β kit	Meso Scale Diagnostics LLC	Cat# K152QPD-1
MSD ultrasensitive mouse/rat insulin kit	Meso Scale Diagnostics LLC	Cat# K152BZC
IL-1ra/IL-1F3; Quantikine ELISA kit	Bio-Techne, Switzerland	Cat#MRA00
Nucleo Spin RNA II kit	Machery Nagel	Cat# 740,955.250
GoScript Reverse transcription Mix using random primers	Promega	Cat# A2801
GoTaq qPCR Master Mix	Promega	Cat# A600A
ReliaPrep™ RNA cell MiniPrep System	Promega	
Il1r1	Applied Biosystems	Mm00434237_m1
Il1b	Applied Biosystems	Mm00434228_m1
Il1a	Applied Biosystems	Mm00439621_m1
Il1rn	Applied Biosystems	Mm00446185_m1
Il6	Applied Biosystems	Mm00446190_m1
Cxcl1	Applied Biosystems	Mm00433859_m1
Cd68	Applied Biosystems	Mm03047340_m1
Emr1	Applied Biosystems	Mm00802529_m1
Gadph	Applied Biosystems	Mm99999915_g1
Actb	Applied Biosystems	Mm00607939_s1
18S	Applied Biosystems	Hs99999901_s1

Continued

REAGENT or RESOURCE	SOURCE	IDENTIFIER
Experimental models: Organisms/strains		
C57BL/6NCrl mice	Inhouse breeding, (originated from Charles River Germany)	MGI:2683688; Strain Code 027; RRID:IMSR_CRL:027
Il1b−/− (B6N.B6-Il1b<tm1Boe>)	Inhouse breeding	N/A
Lyz2-Cre_Il1bfl/fl (B6N.Cg-Lyz2<tm1(cre)Ifo> x B6N.B6-Il1b<tm1Boe)	This manuscript, Lyz2-Cre mouse backcrossed for 10 generations to C57BL/6NCrl prior to intercrossing with B6N.B6-Il1b<tm1Boe	N/A
RIPcre mice (B6-Tg(Ins2-cre)Herr	P. Herrera, backcrossed for 10 generations to C57BL/6NCrl this manuscript	N/A
B6.129X1-Gt(ROSA)26Sortm1(EYFP)	Jackson laboratory, this manuscript backcrossing for 10 generations to C57BL/6NCrl	stock number 006148
(B6-Tg(Ins2-cre)Herr_ B6.129X1-Gt(ROSA)26Sortm1(EYFP)	This manuscript, Inhouse breeding	N/A
Oligonucleotides		
Ins2 forward TGGCTTCTTCTACACACCCAAG	Microsynth	N/A
Ins2 reverse ACAATGCCACGCTTCTGCC	Microsynth	N/A
Pdx1 forward CCCCAGTTTACAAGCTCGCT	Microsynth	N/A
Pdx1 reverse CTCGGTTCCATTCGGGAAAGG	Microsynth	N/A
Gcg forward TTACTTTGTGGCTGGATTGCTT	Microsynth	N/A
Gcg reverse AGTGGCGTTTGTCTTCATTCA	Microsynth	N/A
E2f1 forward TAGCCCTGGGAAGACCTCAT	Microsynth	N/A
E2f1 reverse CCCCAAAGTCACAGTCAAAGAG	Microsynth	N/A
Ccnd1 forward GCGTACCCTGACACCAATCTC	Microsynth	N/A
Ccnd1 reverse CTCCTCTTCGCACTTCTGCTC	Microsynth	N/A
Mki67 forward ATCATTGACCGCTCCTTTAGGT	Microsynth	N/A
Mki67 reverse GCTCGCCTTGATGGTTCCT	Microsynth	N/A
Kir6.2 forward AAGGGCATTATCCCTGAGGAA	Microsynth	N/A
Kir6.2 reverse TTGCCTTTCTTGGACACGAAG	Microsynth	N/A
m18s forward GGGAGCCTGAGAAACGGC	Microsynth	N/A
m18s reverse GGGTCGGGAGTGGGTAATTT	Microsynth	N/A
Hprt forward TCAGTCAACGGGGGACATAAA	Microsynth	N/A
Hprt reverse GGGGCTGTACTGCTTAACCAG	Microsynth	N/A
Gadph foreward AGGTCGGTGTGAACGGATTTG	Microsynth	N/A
Gadph reverse TGTAGACCATGTAGTTGAGGTCA	Microsynth	N/A
Actb foreward GGCTGTATTCCCCTCCATCG	Microsynth	N/A

Continued

REAGENT or RESOURCE	SOURCE	IDENTIFIER
Actb reverse CCAGTTGGTAACAATGCCATGT	Microsynth	N/A
Primers for Il1b−/− genotyping: P1, 5'-TGAGAGCCTGTTGGGTGATCTCCG-3'	Microsynth	N/A
Primers for *Il1b*−/− genotyping: P2, 5'-CACAGCCACAATGAGTGATACTGC-3'	Microsynth	N/A
Primers for *Il1b*−/− genotyping: P3 5'-CAACGGGTTCTTCTGTTAGTCC-3'	Microsynth	N/A
Primers for *Il1b*fl/- genotyping: P1, 5'-GCTACAGAATCTAGTCCTTAGC-3'	Microsynth	N/A
Primers for *Il1b*fl/- genotyping: P2, 5'-CACTTTGTACAAGAAAGCTGG-3'	Microsynth	N/A
Primers for *Il1b*fl/- genotyping: P3, 5'-TGCCTCACTGTATAATTAGACC-3'	Microsynth	N/A
Software and algorithms		
FACS Diva software	BD Biosciences	https://www.bdbiosciences.com
FlowJo (version 10.5.2)	Tree Star	https://www.flowjo.com/solutions/flowjo/downloads
Fiji-ImageJ		https://imagej.net/software/fiji/
GraphPad Prism (version 9.1.0)	Graphpad Prism	https://www.graphpad.com
Other		
Chow diet	Kliba Nafag	3436.EX.F12
Glucose measurement strips FreeStyle Lite	Abbott Diabetes Care Inc	70918-70

RESOURCE AVAILABILITY

Lead contact

Further information and requests for resources and reagents should be directed and will be fulfilled by the lead contact, Marianne Böni-Schnetzler (marianne.boeni@unibas.ch).

Materials availability

Mouse lines generated in this study are available upon request from the lead contact.

Data and code availability

Data

All data reported in this paper will be shared by the lead contact upon request.

Code

This paper does not report original code.

Any additional information required to reanalyze the data reported in this paper is available from the lead contact upon request.

EXPERIMENTAL MODEL AND SUBJECT DETAILS

Experimental animals

C57BL/6NCrl mice. For the time course of IL-1 family gene expression in islets we used 12, 29, 52 and 67-week-old male C57BL/6NCrl mice from our in-house breeding. All mice stemmed from the same breeding

colony and were kept in the same room until islet isolation. Islets of mice with different ages were isolated in parallel on the same day.

IL-1beta ko and myeloIL-1beta ko mice. IL-1beta and myeloIL-1beta ko mice were produced from EUCOMM cells carrying a knockout-first and conditional-ready-allele of IL-1beta (Dror et al., 2017). Briefly, the IL-1beta knockout mice contained 2 homozygous *Il1b* alleles with *loxP* sites flanking exons 4 and 6 and an FRT-LacZ-loxP-neo-FRT cassette between exon 3 and exon 4 (C57BL/6N-Il1b < tm1Boe>) and were termed IL-1beta ko mice. These resulting mice were on a C57BL/6N background and the line was maintained over several generations as heterozygous mice by always crossing them with C57BL/6NCrl mice. To produce homozygous IL-1beta ko (ko/ko) and littermate wildtype (wt/wt) mice for experiments, we intercrossed these heterozygous IL-1beta ko/wt mice to produce IL-1beta ko/ko mice and wt/wt littermate mice as controls. For genotyping the following primers were used: P1, 5′-TGAGAGCCTGTTGGGT GATCTCCG-3′, P2, 5′-CACAGCCACAATGAGTGATACTGC-3′, P3 5′-CAACGGGTTCTTCTGTTAGT CC-3′. The polymerase chain reaction (pcr) products were 311 bp for the transgenic allele and 483 for the wt allele.

To generate the conditional-ready-allele, the IL-1beta ko mouse was crossed with a Flp deleter mouse (also on a C57BL/6N background) to remove the FRT-LacZ-loxP-neo-FRT cassette resulting in mice with an IL-1beta flx allele (*Il1b*^fl/-^ mice). The resulting colony of mice was maintained by crossing to wild-type C57BL/6NCrl mice. For genotyping the following primers were used: P1, 5′-GCTACAGAATCTAGTCCT TAGC-3′, P2, 5′-CACTTTGTACAAGAAAGCTGG-3′ and P3, 5′-TGCCTCACTGTATAATTAGACC-3′. The pcr results in a 676 bp-long product for the transgenic allele (from P1 and P3) and a 519 bp product for the wt allele (from P1 and P2). MyeloIL-1beta ko mice were produced by crossing *Lyz2 Cre*^+/-^ mice (Clausen et al., 1999) backcrossed for more than 10 generations to a C57BL/6NCrl background with *Il1b*^fl/fl^ mice to result in *Lyz2 Cre*^+/-^_ *Il1b*^fl/fl^ mice termed in the following myeloIL-1beta ko mice. Littermate Cre recombinase-negative *Lyz2 Cre*^-/-^_*Il1b*^fl/fl^ mice served as wt controls. *Lyz2 Cre*^+/-^_ *Il1b*^wt/wt^ and littermate *Lyz2 Cre*^-/-^_ *Il1b*^wt/wt^ mice were used for Cre-only control experiments.

RIP-EYFP mice. To produce a mouse line with labeled beta cells for FACS purification, we crossed mice homozygous for loxP-flanked STOP sequence followed by the Enhanced Yellow Fluorescent Protein gene (EYFP) inserted into the *Gt(ROSA)26Sor* locus (B6.129X1-*Gt(ROSA)26Sor*^tm1(EYFP)Cos^, The Jackson laboratory stock number 006148) (Srinivas et al., 2001) with homozygous RIPcre mice (B6-Tg(Ins2-cre)^Herr^, kindly provided by P. Herrera (Herrera et al., 2002). Both lines were completely backcrossed onto a C57BL/6NCrl genetic background prior to intercrossing. This results in double-transgenic mice containing hemizygous alleles of both transgenes.

Animal husbandary

All mice were kept in individually ventilated cages on a 12-hour light and 12-hour dark cycle, fed chow diet (3436.EX.F12, Kliba Nafag, Switzerland) and were allowed to age in our SPF animal facility until the start of the experiments. For all experiments at least two male cohorts were used with littermates as controls. Male mice were used because they develop age-related obesity and glucose intolerance while female mice are protected. Single housing of mice was only used when an aggressive male had to be removed from a cage. Since wt controls and knockout mice were littermates and weaned together into the same cage, no extra group assignment was required. All animal experiments were done according to the Swiss veterinary law and institutional guidelines and were approved by Swiss authorities (Cantonal Veterinary office, Basel-Stadt).

METHOD DETAILS

Glucose and insulin tolerance tests

To determine intraperitoneal glucose tolerance (ipGTT), mice were fasted for 6 hours (from 8 am until 2 pm). Glucose was i.p. injected at a dose of 2g/kg of body weight and blood glucose concentrations were measured at the indicated times using a glucometer (Freestyle, Abbott Diabetes Care Inc.). At time points 0, 15 and 30 minutes after glucose injection, blood was collected from the tail vein for later determination of plasma insulin. To determine insulin tolerance (ipITT), mice were fasted for 3 hours (from 10am until 1pm) followed by i.p. injection of 2U (units)/kg of body weight insulin (Novo Nordisk, Basvaerd, Denmark). Plasma glucose was measured at the indicated time points.

Mouse islet isolation

Islets from male mice with different ages were isolated in parallel by collagenase digestion. Islets were harvested by handpicking under a microscope and 2 h after isolation, islets were collected for RNA extraction (70–80 islets/sample) or cultured in a cell culture incubator (37°C and 5% C0$_2$) in mouse islet media (RPMI-1640 containing 11.1 mM glucose, 100 U/ml penicillin, 100 μg/mL streptomycin, 2 mM glutamax, 50 μg/mL gentamycin, 0.25 μg/mL Amphotericin B and 10% FBS; GIBCO, ThermoFisher Scientific).

Isolation of islet beta and immune cells from 12- and 52-week-old mice by FACS

All mice used for islet isolation stem from our own breeding colony and were kept in the same room. Islets from 12- and 52-week-old RIP-EYFP mice were isolated in parallel on the same day and with the same collagenase solution and cultured in islet media (RPMI-1640 containing 11.1 mM glucose, 100 U/ml penicillin, 100 μg/mL streptomycin, 2 mM glutamax, 50 μg/mL gentamycin, 0.25 μg/mL Amphotericin B and 10% FCS, all reagents were from GIBCO, ThermoFisher Scientific) in a cell culture incubator (37°C and 5% C0$_2$). The next day, islets were washed in PBS and resuspended in a 0.5% trypsin + EDTA solution (GIBCO, ThermoFisher Scientific) at a final concentration of 0.01%. For dispersion of islets into single cells, samples were incubated at 37°C for 90 s, with mechanic up and down pipetting every 30 s. Trypsin activity was stopped by filling the tube with ice-cold FACS buffer (PBS +0.5% BSA + 2mM EDTA). Then cells were washed, resuspend in 100 μL FACS buffer and processed for staining and FACS sorting. To avoid unspecific binding, cells were incubated at 4°C for 15 min with anti-CD16/CD32 (eBioscience, San Diego, CAS, USA), then with anti-mouse CD45 APC antibody (eBioscience, San Diego, CAS, USA) for 30 min on ice. After staining, cells were further processed on a FACSAria III (BD Biosciences) using FACS Diva software (BD Biosciences). Singlet beta cells with EYFP staining were sorted using the YFP channel, the immune cell fraction was collected as CD45+ YFP- cells, and the remaining singlet islet cells were collected as the rest cell fraction. After the sorting, cells were centrifuged and dissolved in lysis buffer (BL Buffer + Thioglycerol, Promega, Madison, USA), and kept at −80°C until RNA extraction using the ReliaPrep RNA cell MiniPrep System (Promega, Madison, USA). In case of beta cells, each experimental unit (n) corresponds to cells from one mouse, in case of islet immune cells and rest cells each n corresponds to cells from one mouse or in some cases to a cell pool derived from 2 mice (in cases where the yield was too low for RNA isolation). The mean number of singlet islet cells per mouse isolated by FACS was 564 ± 100 for CD45 + cells, 16'166 ± 1822 for beta cells and 9810 ± 1408 for rest cells. There was no difference in mean cell yields obtained by FACS from 12-and 52-week-old mice in CD45 + fractions and in respective beta cell fractions (data not shown). Beta cells from C57BL/6NCrl mice or myeloIL-1beta ko mice were sorted based on size and granularity as described before (Dalmas et al., 2017).

Treatment of isolated islets with IL-1beta

For experiments with IL-1beta treatment prior to dispersion into single cells, islets isolated from 29 to 32-week-old male RIP-EYFP mice were cultured for 16 h in mouse islet media with or without 1ng/ml of recombinant mouse IL-1beta (Bio-Techne, Switzerland), followed by dispersion and FACS purification as described above.

Isolation of peritoneal cells to determine IL-1beta protein release

Upon sacrifice the peritoneum of mouse was perfused with 5 mL of PBS containing 1% FCS (GIBCO, ThermoFisher Scientific). The lavage was passed through a 70 um cell strainer (Corning, 431,751) and centrifuged for 10 min at 4°C at 350 x g. Cells were resuspended in culture medium (RPMI-1640 containing 11.1 mM glucose, 100 U/ml penicillin, 100 μg/mL streptomycin, 2 mM glutamax, 50 μg/mL gentamycin, 0.25 μg/mL Amphotericin B and 10% FBS; GIBCO, ThermoFisher Scientific) and 250'000 cells/well were cultured overnight in 250 ul of medium. Non-adherent cells were washed away and adherent peritoneal cells were treated for 16 h with or without LPS at a concentration of 100 ng/mL (InvivoGen, tlrl-smlps, LPS from S. minnesota R595). If indicated ATP (InvivoGen, tlrl-atp) was added at a concentration of 5 mM for 60 min prior to collection of culture supernatants. IL-1beta concentrations in cell culture supernatants were measured using MSD mouse IL-1beta assay kit (K152QPD; Meso Scale Discovery) according to the "alternative protocol 2" of the manufacturer's instructions (LLOD = 0.11 pg/mL).

Glucose-stimulated insulin secretion assay of isolated islets

Following overnight recovery, islets were pre-incubated for 90 min in preequilibrated Krebs-Ringer bicarbonate buffer (KRB; 115 mM NaCl, 4.7 mM KCl, 2.6 mM CaCl$_2$ 2H$_2$O, 1.2 mM KH$_2$PO$_4$, 1.2 mM MgSO$_4$ 7H$_2$O,

10 mM HEPES, 0.5% bovine serum albumin, pH 7.4) containing 2.8 mM glucose. Borosilicate tubes with 1 mL KRB with 2.8 mM or 16.7 mM glucose were prepared and 10 islets were added per tube (3–4 replicates per mouse and per condition). Islets were incubated in a heating cabinet at 37°C and 0.5 mL of the islet supernatant was collected 60 min later. To determine islet insulin content, 0.5 mL of 0.5 N HCL/EtOH was added to each tube, followed by vortexing and incubation for 1h at −20°C. Supernatants were collected and stored at −20°C for later insulin measurements. The extracted insulin content was expressed as mean amount of insulin in ng per islet (means per mouse were calculated from 3-4 replicates with 10 islets each).

Hormone and cytokine detection

Insulin and IL-1beta concentrations were determined using the ultrasensitive mouse/rat insulin and the IL-1beta assay (Meso Scale Diagnostics LLC, Rockville, MD). IL-1Ra was measured in plasma obtained by cardiac puncture at sacrifice with the IL-1ra/IL-1F3; Quantikine ELISA kit (Bio-Techne, Switzerland).

Determination of beta cell mass and islet area from IL-1beta ko and myeloIL-1beta ko mice and respective littermate controls

The weight of the pancreas was determined at sacrifice. To measure the beta cell mass and mean islet area, pancreata of IL-1beta and myeloIL-1beta ko mice and their respective littermate control mice were fixed in 4% buffered formalin at 4°C overnight and embedded in paraffin. Organs were cut with an electronic rotary Microtome, Microm HM 340E. As soon as a representative area of the organ was reached, five 5-μm-thick sections were collected. Thereafter, 100 μm were trimmed and then again five 5-μm-thick sections were collected. This was repeated so that in the end three to four representative sections from different depths of the pancreas could be further deparaffinised and re-hydrated. For insulin staining, the slides were incubated with a guinea pig anti-insulin antibody (Dako, A0564) for 2h at room temperature, followed by an overnight staining at 4°C with a rat anti-CD45 antibody (BD Pharmingen, 550539) to detect lymph nodes. The next day, the slides were incubated consecutively with Alexa Fluor 647-conjugated goat anti–guinea pig IgG (Invitrogen, A21450) and Alexa Fluor 555-conjugated goat anti-rat IgG (Invitrogen, A21434), each for 2h. Cell nuclei were stained with DAPI and sections were mounted with mounting medium (Dako, S3023). For image acquisition a Prior PL-200 slide loading robot and an automated Nikon Eclipse Ni microscope with a Hamamatsu flash 4.0 camera and a 4x Nikon Objective NA 0.2 was used.

Image analysis was performed using ilastik (Berg et al., 2019), which was trained to segment the pancreas area of stitched multichannel images, including channels for DAPI nuclei, GFP for autofluorescence, Alexa 555 for lymph nodes and Alexa 647 for insulin.

The simple segmentation outputs of ilastik and corresponding original multichannel images were subsequently processed using Fiji (Schindelin et al., 2012). In a first step, the ilastik simple segmentation recognition of the pancreas was controlled and corrected manually if needed. In a second step, the beta cell identification on the corresponding channel (stained with Alexa 647) was obtained by setting all pixels that do not overlap with the pancreas area to 0, thresholding using the Otsu method and preforming a connected component analysis on objects bigger than 900 μm^2 and having a circularity value bigger than 0.2. Beta cell object recognition was adjusted manually if needed. The Fiji analysis workflow was facilitated using a custom ImageJ script, which is available upon request. The pancreas area was obtained by subtraction of the lymph node area (CD45 + area). The mean % insulin positive area of the pancreas area was determined from three to four pancreas sections per mouse. This mean % insulin positive area and the total pancreas weight was used to calculate the beta cell mass (mg).

Determination of Ki67 + beta cells in histology sections from IL-1beta ko and littermate control mice

Formalin-fixed pancreata embedded in paraffin were cut into 5-μm-thick sections, deparaffinized, rehydrated and stained. Ki67/insulin/DAPI triple fluorescence staining was done as described before (Böni-Schnetzler et al., 2018). Briefly, upon heat-induced antigen retrieval sections were stained overnight with a biotinylated anti-Ki67 antibody (13–5698 from e-bioscience) at 4°C followed by insulin staining with a guinea pig anti-insulin Ab (DAKO A0564). This was followed by a streptavidine-coupled fluorochrome (DyLight549, Adipogen AG) and Fluorescein (FITC) AffiniPure F(ab')₂ Fragment Donkey Anti-Guinea Pig IgG (Jackson Immuno Research Laboratories, West Grove PA). DAPI (SIGMA) was used to label nuclei. Stained sections were mounted in fluorescence mounting medium (DAKO). Pictures of stained pancreas

sections were acquired with a Nikon TI2 microscope equipped with CFI Plan Apo Lambda objectives (4X and 20X), connected to a Photometrics Prime 95B (for fluorescence imaging, Teledyne Photometrics, USA) and using the Nikon NIS software. For analysis, images were visualized using Fiji/ImageJ software (NIH, USA), and Ki67 + ins + double-positives cells were counted manually. To determine the number of Ki67 + ins + islet cells in IL-1beta ko and wt mice an average number of 98.1 $\pm$ 20.82 islets per mouse were analyzed.

RNA extraction and qPCR

Total RNA of mouse islets or liver was extracted using the Nucleo Spin RNA II Kit (Machery Nagel, Düren, Germany). For FACS-isolated islet cells, the ReliaPrep RNA Cell Miniprep System (Z6011, Promega) was used. cDNA was prepared with the GoScript Reverse Transcription Mix containing random primers (Promega AG, Dübendorf, Switzerland) according to the manufacturer's instructions. For quantitative PCR of IL-1 family and inflammation gene expression the highly specific and sensitive Applied Biosystems TaqMan real-time PCR assays (Applied Biosystems) were used. For all other genes, SYBRgreen-based chemistry with GoTaq Polymerase (Promega AG, Dübendorf, Switzerland) and the ABI 7500 fast system (Applied Biosystems) was employed. TaqMan assays and primers for SYBR green qPCRs are described in the Key Resources Table. For normalization of qPCR the geometrical mean of *Actb*, *Hprt* and *Gadph* was used. Relative gene expression was calculated with the comparative $2^{-\Delta\Delta CT}$ method (Schmittgen and Livak, 2008).

QUANTIFICATION AND STATISTICAL ANALYSIS

Results were analyzed with Prism 9.1.0 (GraphPad, USA) and $p < 0.05$ was considered to be significant. Results were expressed as mean $\pm$ SEM. Data were analyzed with unpaired Student's t test or with one-way or two-way ANOVA and Sidak's multiple comparison test. Statistical details of experiments can be found in the figure legends and in the figures.